

# 000 001 002 003 004 005 006 007 008 009 010 011 012 013 014 015 016 017 018 019 020 021 022 023 024 025 026 027 028 029 030 031 032 033 034 035 036 037 038 039 040 041 042 043 044 045 046 047 048 049 050 051 052 053 UNLEARNING WITH ASYMMETRIC SOURCES: IMPROVED UNLEARNING-UTILITY TRADE-OFF WITH PUBLIC DATA

Anonymous authors

Paper under double-blind review

## ABSTRACT

Achieving certified data erasure in machine unlearning faces a fundamental trade-off: preserving model utility requires less noise, but formal privacy guarantees demand more. This tension typically degrades model performance. In this work, we study this challenge in Langevin Unlearning, a noisy variant of SGD that is uniquely amenable to theoretical analysis. We introduce an asymmetric unlearning setting assuming that datasets contain both private data (subject to unlearning) and public data (permanently retained). Our framework demonstrates that incorporating public data enables better unlearning-utility trade-offs without additional noise or restrictive differential privacy assumptions. We prove that public data volume quadratically reduces the Rényi divergence between unlearning and re-training distributions, allowing control over unlearning guarantees through data composition rather than noise amplification. The framework also provides a fine-grained analysis of how distributional alignment between public and private data affects performance preservation. Empirical validation using variational Rényi divergence estimation confirms our theoretical predictions, showing that strategic public data injection achieves comparable unlearning efficacy while significantly improving model performance and computational efficiency.

## 1 INTRODUCTION

The widespread adoption of machine learning across diverse applications has prompted regulatory responses aimed at protecting user privacy and data rights. Legislative frameworks such as the European Union’s AI Act (Parliament & of the European Union, 2024) and Canada’s Artificial Intelligence and Data Act (AIDA) (Parliament of Canada, 2022) establish fundamental principles including the “right to be forgotten”, which mandates that individuals can request removal of their personal data from trained systems. This requirement presents significant technical challenges for modern machine learning paradigms, particularly deep learning and generative AI models that depend on large-scale datasets collected from public sources, often without explicit individual consent. Compounding this challenge, recent research demonstrates that neural networks exhibit a propensity to memorize training examples while maintaining generalization performance (Attias et al., 2024; Carlini et al., 2022; Nasr et al., 2023; Zhang et al., 2016).

The most straightforward approach to addressing data removal requests would be to retrain models from scratch after excluding the specified data points. However, this naive solution becomes prohibitively expensive for contemporary large-scale models, where training can require substantial computational resources. Moreover, the frequency of such requests in production systems would render this approach operationally impractical. This reality necessitates the development of machine unlearning techniques that can selectively remove specific data points from trained models while preserving overall performance. For certain applications, such removal should be certifiable through formal guarantees, ensuring that the unlearned model is statistically indistinguishable from one that was never trained on the removed data. Thus, effective unlearning algorithms must satisfy three fundamental requirements: provable erasure of target data, preservation of model utility, and computational efficiency that outperforms full retraining.

054 Most existing machine unlearning approaches operate under the assumption that *any* data point  
 055 in the training set may require removal. While this assumption holds when working exclusively  
 056 with sensitive datasets, it proves overly restrictive for real-world scenarios. Modern data collection  
 057 pipelines aggregate information from heterogeneous sources, combining both sensitive private data  
 058 and publicly available content. CommonCrawl (Common Crawl Foundation, 2024) and ImageNet  
 059 (Deng et al., 2009) are examples of publicly available data used to train large language models  
 060 and vision models. To our knowledge, the only prior work exploring mixed-privacy unlearning is  
 061 Golatkar et al. (2021), who introduced Mixed-Linear Forgetting for computer vision tasks. Their  
 062 approach requires architectural modifications to achieve forgetting through network linearization,  
 063 limiting its general applicability. In the privacy-preserving machine learning literature, several works  
 064 have shown that having access to a set of public data points allows for the design of algorithms  
 065 with better privacy guarantees for the same amount of noise introduced into the model. When the  
 066 public data distribution is close enough to the sensitive data distribution, these public data-assisted  
 067 algorithms often offer a better privacy-utility trade-off than their conventional counterparts (Alon  
 068 et al., 2019b; Amid et al., 2022; Ganesh et al., 2023a; Lowy et al., 2024).

069 In this work, we study the effect of considering that a portion of the training dataset is public  
 070 and never subject to unlearning. We study this setting under Langevin Unlearning (Chien et al.,  
 071 2024a), showing that restricting unlearning to private data improves guarantees. We ask the ques-  
 072 tions: **(1) Does adding public data improve Langevin Unlearning performance?** **(2) How does**  
 073 **public-private distribution mismatch affect post-unlearning performance?** Our theoretical analy-  
 074 sis provides clear answers. We first prove that injecting public data creates a more favorable initial-  
 075 ization for the unlearning process (Theorems 3.1 and 3.2). We then provide a fine-grained analysis  
 076 of the unlearning-utility trade-off, with our main contribution stated in Theorem 3.3, explaining how  
 077 the distributional alignment between public and private data impacts the model’s final performance.  
 078 Finally, building on a variational representation of Rényi divergence (Birrell et al., 2023), we de-  
 079 velop in Section 4.1 a framework for numerical evaluation of our bounds, showing that they capture  
 080 some of the key dynamics of private-public learning and unlearning in practical settings.

## 082 2 BACKGROUND AND NOTATION

### 084 2.1 MACHINE UNLEARNING

086 Machine unlearning algorithms eliminate the influence of designated training data (the *forget set*)  
 087 while balancing unlearning efficacy, model utility, and computational efficiency. Three canonical  
 088 strategies illustrate the trade-offs: random re-initialization achieves perfect unlearning but destroys  
 089 utility; retraining from scratch provides optimal guarantees but incurs prohibitive costs; no intervention  
 090 preserves utility but achieves no unlearning. This motivates two paradigms: **Exact unlearning**  
 091 replicates the retraining baseline through specialized architectures like SISA (Bourtoule et al., 2020)  
 092 or Arcane (Yan et al., 2022), which enable targeted retraining but increase complexity. **Approximate**  
 093 **unlearning** tolerates bounded discrepancies from retraining for practicality, including Newton-step  
 094 updates (Golatkar et al., 2020) and noisy fine-tuning schemes like Langevin Unlearning (Chien et al.,  
 095 2024a;b).

### 097 2.2 NOTATION

099 We consider probability distributions defined over a compact parameter space  $\Theta$ , where stochastic-  
 100 ity arises from three sources: the weight initialization distribution  $\pi_0$ , the training data distribution  
 101  $P_{\text{train}}$ , and the inherent randomness of the optimization procedure. We denote by  $\mathcal{P}(\Theta)$  the set of  
 102 probability distributions supported on  $\Theta$ . Our analysis focuses on three parameter distributions:  $\pi_L^T$   
 103 (the learning distribution after  $T$  iterations of training on the full dataset),  $\pi_U^K$  (the unlearning dis-  
 104 tribution after  $K$  iterations of the unlearning procedure), and  $\pi_R^T$  (the retraining distribution after  $T$   
 105 iterations of training only on the retain set). A key quantity in our analysis is the Rényi divergence  
 106 of order  $\alpha$  between distributions  $P$  and  $Q$ , denoted  $D_\alpha(P\|Q)$ , which we define rigorously in sub-  
 107 sequent sections. We use  $P_{\text{pub}}$  and  $P_{\text{priv}}$  to represent the distributions of public and private data,  
 108 respectively.

108  
109 2.3 LANGEVIN UNLEARNING110 A common approach to machine unlearning is to run a noisy projected gradient method starting  
111 from the trained weights, targeting a distribution close to retraining. Formally, at iteration  $t$ ,

112  
113 
$$\theta_{t+1} = \Pi_{\Theta}[\theta_t - \eta \nabla_{\theta} \mathcal{L}(\theta_t) + \xi_t], \quad (1)$$

114 where  $\mathcal{L}$  is a surrogate loss (e.g., empirical loss on a retain set),  $\eta$  is the step size, and  $\xi_t$  is injected  
115 noise (often Gaussian) controlling distributional closeness.116 Langevin Unlearning (LU) (Chien et al., 2024a) instantiates this scheme with  $\mathcal{L} = \mathcal{L}_{\mathcal{D}_r}$ , the loss on  
117 the retain set, and  $\xi_t \sim \mathcal{N}(0, 2\eta\sigma^2 I_d)$ . This reduces to projected noisy gradient descent (PNGD)  
118 (pseudocode in Appendix A.5):

119  
120 
$$\theta_{t+1} = \Pi_{\Theta} \left[ \theta_t - \eta \nabla_{\theta} \mathcal{L}_{\mathcal{D}_r}(\theta_t) + \sqrt{2\eta\sigma^2} W_t \right], W_t \sim \mathcal{N}(0, I_d) \quad (2)$$

121  
122 LU provides certifiable approximate unlearning guarantees by minimizing the Rényi divergence be-  
123 tween post-unlearning and post-retraining weight distributions (Chien et al., 2024a;b). However,  
124 these guarantees require that the *entire original training process* satisfies differential privacy (DP),  
125 necessitating PNGD with substantial noise injection from initialization. This requirement limits  
126 practical applicability, as it degrades model performance both before and after unlearning. In this  
127 work, we improve upon Chien et al. by relaxing the global DP assumption. Rather than requiring  
128 the entire learning process to satisfy DP, we assume only that the initialization distribution satisfies  
129 a log-Sobolev inequality—a mild condition naturally satisfied by standard Gaussian initialization.  
130 This property is preserved through PNGD iterations by Lemma A.1 due to loss smoothness. This  
131 relaxation enables us to derive data-dependent bounds that quantify how public data abundance  
132 improves unlearning without noise amplification, a key contribution unavailable in prior work. Con-  
133 current approaches like (Koloskova et al., 2025) require only smoothness assumptions, but such  
134 data-agnostic bounds depend primarily on projection set geometry rather than training data struc-  
135 ture.136 3 ASYMMETRIC LANGEVIN UNLEARNING  
137138 **Motivation.** Our approach is motivated by a realistic data setting, well-established in the privacy-  
139 preserving machine learning literature, that leverages public data to improve the privacy-utility trade-  
140 off (Alon et al., 2019a; Ganesh et al., 2023b; Lowy et al., 2024; Amid et al., 2022). We introduce  
141 this asymmetric data model to Langevin Unlearning, which allows us to relax the restrictive Dif-  
142 fferential Privacy (DP) assumption over the entire dataset. By explicitly modeling this asymmetry,  
143 we can leverage public data to enhance the unlearning process to improve both efficacy and model  
144 performance without compromising privacy guarantees.145 **Problem Setting.** We consider empirical risk minimization over a dataset  $D = D_{\text{pub}} \cup D_{\text{priv}}$   
146 comprising two components: a public set  $D_{\text{pub}}$  with  $n_{\text{pub}}$  samples from a distribution  $P_{\text{pub}}$ , and  
147 a private set  $D_{\text{priv}}$  with  $n_{\text{priv}}$  samples from a distribution  $P_{\text{priv}}$ . The training loss is  $\mathcal{L}_D(\theta) =$   
148  $\frac{1}{n_{\text{pub}}+n_{\text{priv}}} \sum_{x \in D} l(\theta, x)$ . Only the private data is subject to unlearning requests, while public data  
149 remains permanently available. We employ  $T$  PNGD iterations with projections onto  $\Theta \subset \mathbb{R}^d$   
150 (radius  $R$ ) to obtain  $\theta_T$ . Since PNGD injects Gaussian noise at each step, it induces probability  
151 distributions over parameters rather than deterministic iterates. In order to ensure that everything is  
152 well-behaved, one has to impose a regularity assumption on the initialization probability distribution.153 **Definition 3.1.** (Log-Sobolev inequality (Gross, 1975)) A probability measure  $P \in \mathcal{P}(\mathbb{R}^d)$  satisfies  
154 a Log-Sobolev inequality with constant  $C$  if

155  
156 
$$\forall Q \in \mathcal{P}(\mathbb{R}^d), D_{KL}(Q||P) \leq \frac{C}{2} I(Q, P), \quad (3)$$

157 where  $D_{KL}$  denotes the KL divergence and  $I(Q, P) = E_Q \left[ \|\nabla \log \frac{q}{p}\|^2 \right]$  is the relative Fisher  
158 information.159 Our analysis compares two such distributions: the *unlearning distribution*  $\pi_U$  (obtained by applying  
160 LU on the retain set from the trained model), and the *retraining distribution*  $\pi_R$  (obtained by training

from scratch on the retain set). Following Chien et al. (2024a), we measure unlearning quality via Rényi divergence.

**Definition 3.2.** For probability measures  $P, Q$  with  $P \ll Q$ , their Rényi divergence of order  $\alpha \in (0, +\infty) \setminus \{1\}$  is

$$D_\alpha(P\|Q) = \frac{1}{\alpha-1} \log \mathbb{E}_Q \left[ \left( \frac{dP}{dQ} \right)^\alpha \right],$$

where  $\frac{dP}{dQ}$  is the Radon-Nikodym derivative. This generalizes KL divergence ( $\alpha \rightarrow 1$ ), reverse-KL ( $\alpha \rightarrow 0$ ), and connects to  $\varepsilon$ -differential privacy in the limit  $\alpha \rightarrow \infty$  (Mironov, 2017).

**Our Contribution.** Our main contribution is showing that incorporating public data improves the unlearning-utility trade-off. While prior work proved that Langevin Unlearning’s efficacy increases with noise magnitude (Chien et al., 2024a;b), this approach often degrades model performance. We break this dependency by introducing a new lever: the volume of public data. We demonstrate that increasing the amount of public data improves unlearning guarantees, i.e., lowers the Rényi divergence  $D_\alpha(\pi_U\|\pi_R)$ , without requiring additional noise injection or a global DP assumption. This allows for a fine-grained control over unlearning by adjusting data composition rather than simply amplifying noise.

### 3.1 DEFINING THE WEIGHT DISTRIBUTIONS

Consider the PNGD learning algorithm  $\mathcal{A}$  applied to dataset  $D = D_{\text{pub}} \cup D_{\text{priv}}$ , where an unlearning request targets a subset  $D_{\text{forget}} \subseteq D_{\text{priv}}$ . Our analysis describes the relationship between three weight distributions arising from different training scenarios:

**Learning distribution  $\pi_L^T$ :** The weight distribution after  $T$  PNGD iterations on the complete dataset  $D$ , starting from  $\theta_0 \sim \pi_0$ , a sample from the initialization distribution  $\pi_0$ . This represents the original trained model before any unlearning requests.

**Unlearning distribution  $\pi_U^K$ :** The weight distribution after  $K$  PNGD iterations on the retain set  $D \setminus D_{\text{forget}}$ , initialized from  $\theta_0 \sim \pi_L^T$ . This captures the model state after applying our unlearning procedure to the originally trained model.

**Retraining distribution  $\pi_R^T$ :** The weight distribution after  $T$  PNGD iterations on the retain set  $D \setminus D_{\text{forget}}$ , starting from the original initialization  $\theta_0 \sim \pi_0$ .

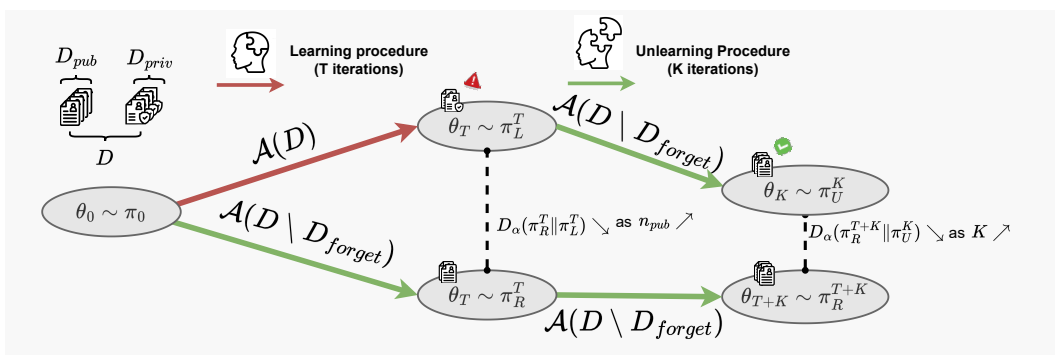


Figure 1: Training pipelines showing the relationship between learning, unlearning, and retraining with public data injection. The divergence  $D_\alpha(\pi_R^T\|\pi_L^T)$  quantifies how public data helps maintain similarity between retraining and original learning distributions, facilitating subsequent unlearning.

The effectiveness of unlearning is measured by  $D_\alpha(\pi_U^K\|\pi_R^{T+K})$ , while the presence of public data helps control  $D_\alpha(\pi_R^T\|\pi_L^T)$ , creating favorable conditions for the unlearning process.

216 3.2 UNLEARNING PERFORMANCE  
217

218 We now present theoretical guarantees for asymmetric Langevin unlearning that demonstrate how  
219 public data fundamentally improves unlearning efficiency. Our analysis adapts the prior work of  
220 Chien et al. (2024a) by removing restrictive differential privacy assumptions, and providing explicit  
221 characterization of how public and private data contributions differ in the unlearning bounds. We  
222 also provide minor corrections to the bounds presented in Chien et al. (2024a); note, however, that  
223 these corrections do not change the key contributions and messages in (Chien et al., 2024a).

224 The following result explains how public data reduces reliance on differential privacy constraints,  
225 decoupling unlearning efficacy from model performance and enabling fine-grained analysis of this  
226 trade-off across different public-private distribution regimes (Section 3.3).

227 **Theorem 3.1** (The role of public data in shrinking the learning / retraining mismatch. ). *Suppose  
228 that the loss is  $L$ -smooth and  $M$ -Lipschitz, and that the initialization distribution satisfies a  $C_0$ -log  
229 Sobolev inequality. Moreover, suppose that the PNGD updates project onto a compact set  $\Theta$  of  
230 radius  $R$ .*

231 *Then at learning iteration  $T$ , we have the following upper bound on the Renyi divergence between  
232 the retraining  $\pi_R^T$  and learning  $\pi_L^T$  distributions:*

$$233 \frac{D_\alpha(\pi_R^T \| \pi_L^T)}{\alpha} \leq \frac{2M^2\eta^2 n_{\text{forget}}^2}{(n_{\text{pub}} + n_{\text{priv}})^2 \sigma^2} \sum_{t=1}^{T-1} \prod_{t'=t}^{T-1} \left(1 + \frac{\eta\sigma^2}{C_{t',1}}\right)^{-1},$$

236 where  $0 < C_{t',1} \leq (1 + \eta L)^{2K} C_0 + 2\eta\sigma^2 \frac{(1 + \eta L)^{2K} - 1}{(1 + \eta L)^2 - 1}$  are log Sobolev constants of the distributions  
237 of the intermediate PNGD updates. Using the support's radius allows to loosely upper bound those  
238 constants (Chien et al., 2024a):  $C_{t',1} \leq 6e^{\frac{4\tau}{\eta\sigma^2}} (4\tau^2 + \eta\sigma^2)$  with  $\tau = R + \eta M$ .  
239

240 *Proof sketch.* The proof follows the analytical framework of Chien et al. (2024a, Theorem 3.3),  
241 adapted to leverage the presence of public data in the training set. By distinguishing between public  
242 and private data contributions in the gradient updates, we reduce the privacy erosion (Chourasia  
243 et al., 2021) of each PNGD update.

244 This bound reveals that we can fix noise magnitude  $\sigma$  to be arbitrarily small to preserve performance  
245 while controlling the divergence through public data volume. When  $n_{\text{pub}} \gg n_{\text{forget}}$ , the learning  
246 and retraining distributions remain close regardless of noise level, providing favorable initial conditions  
247 for unlearning (Fig. 2b). Geometrically, for any fixed forget set size, the retraining distribution  
248 stays within a divergence ball whose radius shrinks quadratically with the number of public points.

249 **Theorem 3.2** (Convergence guarantee of Langevin unlearning (Chien et al., 2024a, Theorem 3.2)).  
250 *Suppose that the loss is  $L$ -smooth and  $M$ -Lipschitz, and that the learning distribution of weights at  
251 time  $T$  satisfies a  $C$  log-Sobolev inequality. Then, the Renyi divergence between  $\pi_U^K$  (the unlearn-  
252 ing distribution after  $K$  iterations) and the retraining distribution after  $T + K$  iterations is upper  
253 bounded by*

$$254 D_\alpha(\pi_R^{T+K} \| \pi_U^K) \leq D_\alpha(\pi_L^T \| \pi_R^T) \min \left( \prod_{k=1}^K \left(1 + \frac{2t\sigma^2}{(1 + \eta L)^2 C_{U,k}}\right)^{\frac{-1}{\alpha}}, \exp\left(-\frac{2K\sigma^2\eta}{\alpha\tilde{C}}\right) \right),$$

257 where  $0 < C_k \leq (1 + \eta L)^{2K} C + 2\eta\sigma^2 \frac{(1 + \eta L)^{2K} - 1}{(1 + \eta L)^2 - 1}$ , and  $\tilde{C} \leq 6(4\tau^2 + 2\eta\sigma^2) \exp\left(\frac{4\tau^2}{2\eta\sigma^2}\right)$ .  
258

259 Moreover, if the loss function is  $m$ -strongly convex and the initial log-Sobolev constant satisfies  $C >$   
260  $\frac{\sigma^2}{m}$ , we get the following exponential decay of the Renyi divergence with respect to the unlearning  
261 iteration:

$$262 D_\alpha(\pi_R^{T+K} \| \pi_U^K) \leq D_\alpha(\pi_L^T \| \pi_R^T) \exp\left(-\frac{2K\sigma^2\eta}{C\alpha}\right).$$

265 This theorem establishes the convergence guarantee for Langevin unlearning by showing that  
266 the Renyi divergence between the unlearning and retraining distributions decreases exponentially  
267 with unlearning iterations  $K$ , with the convergence rate controlled by the initial divergence  
268  $D_\alpha(\pi_R^{T+K} \| \pi_U^K)$ . When combined with Theorem 3.1, this reveals the mechanism by which public  
269 data improves unlearning: the quadratic reduction in initial divergence from public data injection  
translates directly into tighter convergence bounds.

270 3.3 PERFORMANCE WITHOUT NOISE: THE ROLE OF DISTRIBUTION ALIGNMENT  
271

272 LU faces a fundamental dilemma: increasing noise improves unlearning guarantees but degrades  
273 model performance. Our asymmetric approach breaks this trade-off by leveraging public data abun-  
274 dence rather than noise amplification. However, the effectiveness of this strategy depends on the  
275 relationship between public and private data distributions.

276 We now analyze when public data injection preserves performance, and when it introduces new  
277 challenges. Our results reveal that performance preservation is not automatic – it depends on the  
278 distributional alignment between public and private data. When these distributions are similar, pub-  
279 lic data acts as a performance stabilizer, allowing effective unlearning without quality degradation.  
280 Conversely, when distributions differ significantly, performance impacts emerge, though they remain  
281 more controlled than noise-based approaches.

282 We evaluate post-unlearning performance on the private data distribution *only*, reflecting realistic  
283 deployment scenarios where the primary concern is maintaining model quality on the sensitive data  
284 that remains after unlearning. Performance analysis on the full mixture of public and private distri-  
285 butions is provided in Appendix A.4.1 for completeness.

286 **Theorem 3.3.** *Assuming the data generating distributions share the same support, that the weight  
287 space  $\Theta$  is compact and that the loss is  $M$ -Lipschitz wrt  $\theta$ , we have the following upper bound on the  
288 generalization error on the private data after performing  $K$  iterations of unlearning, and initializing  
289 a weight  $\theta_0$  from  $\pi_L^T$ :*

$$\begin{aligned} 291 \mathbb{E}_{\theta \sim \pi_U^K} [\mathbb{E}_{x \sim P_{\text{priv}}} [\mathcal{L}(\theta, x)]] &\leq \underbrace{\exp \left( \frac{n_{\text{pub}}}{n_{\text{pub}} + n_{\text{retain}}} D_{\infty}(P_{\text{priv}} \| P_{\text{pub}}) \right)}_{\text{distribution mismatch penalty}} \mathbb{E}_{\theta \sim \pi_R^{T+K}} [\mathbb{E}_{d \sim P_{\text{train}}} [\mathcal{L}(\theta, d)]] \\ 292 \\ 293 &\quad + M \times \text{diam}(\Theta) \times \underbrace{\sqrt{\frac{1}{2} D_{\alpha}(\pi_R^{T+K} \| \pi_U^K)}}_{\text{unlearning approximation error}}, \end{aligned}$$

294 where  $D_{\infty}(P \| Q) = \log \left( \text{ess sup}_{x \sim Q} \frac{p(x)}{q(x)} \right)$  is the infinite Rényi divergence (worst case regret (Er-  
295 ven & Harremoës, 2014)) and  $P_{\text{train}}$  denotes the mixture of distributions  $D_{\text{pub}}$  and  $D_{\text{priv}}$  used for  
296 training the model.

297 *Proof sketch.* The proof uses the Kantorovitch-Rubinstein duality Theorem A.1 to bound the perfor-  
298 mance gap by the dual of the Wasserstein distance between  $\pi_U^K$  and  $\pi_L^{T+K}$ , then relates this to Rényi  
299 divergence via standard inequalities leveraging the compactness of the weight space  $\Theta$ . For private  
300 data evaluation, importance weighting introduces a mismatch penalty controlled by the worst case  
301 regret,  $D_{\infty}(P_{\text{priv}} \| P_{\text{pub}})$ , weighted by the public data fraction.

302 This proposition enables a fine-grained analysis of the unlearning-performance trade-off. In the  
303 regime where  $n_{\text{pub}} \rightarrow \infty$  (optimal for unlearning efficacy):

- 311 1. **Aligned distributions** ( $D_{\infty}(P_{\text{priv}} \| P_{\text{pub}}) \approx 0$ ): The distribution mismatch penalty van-  
312 ishes, and the unlearned model’s performance on unseen private data is guaranteed to be at  
313 least as good as the retrained model’s performance on the training mixture. This represents  
314 the ideal scenario where public data injection preserves performance.
- 315 2. **Misaligned distributions** ( $D_{\infty}(P_{\text{priv}} \| P_{\text{pub}}) \gg 0$ ): The exponential penalty term domi-  
316 nates, causing the upper bound to become vacuous. While this confirms that performance  
317 degradation will occur, the bound’s looseness prevents us from quantifying the actual ex-  
318 tent of this degradation. The true performance impact may be better than this worst-case  
319 guarantee suggests.

320 **Retraining performance bound** ( $\mathbb{E}_{\theta \sim \pi_R^T} [\mathbb{E}_{x \sim P_{\text{train}}} [\mathcal{L}(\theta, x)]]$ ): The upper bound could be fur-  
321 ther improved to include the *optimal* distribution, i.e by linking  $\mathbb{E}_{\theta \sim \pi_R^T} [\mathbb{E}_{x \sim P_{\text{train}}} [\mathcal{L}(\theta, x)]]$  to  
322  $\arg \min_{\pi \in \mathcal{P}(\mathbb{R}^d)} \mathbb{E}_{\theta \sim \pi} [\mathbb{E}_{x \sim P_{\text{train}}} [\mathcal{L}(\theta, x)]]$ . However, standard generalization bounds for Langevin  
323 dynamics (Raginsky et al., 2017; Xu et al., 2018) do not directly apply to our setting due to the

324 projection operator  $\Pi_\Theta$  in the PNGD updates. These classical results focus on unconstrained non-  
 325 convex optimization, whereas our bounded domain introduces additional complexity. The most relevant  
 326 analysis we are aware of is Lamperski (2020), who study generalization properties of projected  
 327 Stochastic Gradient Langevin Dynamics, though their work considers the infinite-data regime.  
 328

## 329 4 EXPERIMENTS

331 Our theoretical analysis provides upper bounds on the Rényi divergence  $D_\alpha(\pi_R^{T+K} \parallel \pi_U^K)$  that governs  
 332 unlearning performance. However, these bounds involve iteration-dependent log-Sobolev constants  
 333 that are difficult to estimate in practice, making it unclear how tight our theoretical guarantees  
 334 actually are. To gain empirical insight into the behavior of this divergence, we estimate its value  
 335 using samples from the weight distributions. To our knowledge, this is the first attempt to evaluate  
 336 unlearning performance through direct estimation of the Rényi divergence between the parameter  
 337 distributions—moving beyond output-based unlearning evaluations to directly examine the parameter  
 338 distributions. Building on Birrell et al. (2021; 2023), we leverage the variational representation  
 339 of the Rényi divergence for numerical estimation.

340 **Theorem 4.1.** *(Convex conjugate variational approximation of the Rényi divergence (Birrell et al.,  
 341 2023)) Let  $P, Q$  two probability distributions supported on  $\Omega$ , such that  $P \ll Q$ , and let  $\mathcal{M}_b$  be the  
 342 space of bounded measurable functions on  $\Omega$ . Then,  $\forall \alpha \in (0, +\infty) \setminus \{1\}$ ,*

$$343 \frac{D_\alpha(P \parallel Q)}{\alpha} = \sup_{g \in \mathcal{M}_b(\Omega), g < 0} \int g dQ + \frac{1}{\alpha - 1} \int |g|^{\frac{\alpha-1}{\alpha}} dP + \alpha^{-1} (\log \alpha + 1). \quad (4)$$

346 This variational representation of Rényi divergence allows us to obtain estimates of  $D_\alpha(\pi_R^{T+K} \parallel \pi_U^K)$   
 347 using trained models as samples – to our knowledge, the first such attempt in the unlearning literature.  
 348 We emphasize that this is not intended as a practical evaluation methodology for machine  
 349 unlearning, as it requires training numerous models to obtain sufficient samples for reliable estimation.  
 350 Standard approaches like membership inference attacks (MIAs) (Shokri et al., 2017; Carlini et al., 2021; Hayes et al., 2024) remain more suitable for practical evaluation. Our goal is purely  
 351 investigative: to understand how the Rényi divergence behaves empirically and assess whether our  
 352 theoretical bounds, despite containing hard-to-estimate constants, provide meaningful guidance in  
 353 realistic scenarios.  
 354

355 We present our findings in two parts: Sections 4.1 and 4.2 investigate the behaviour of the upper  
 356 bounds provided respectively in Theorem 3.2 and Theorem 3.3, while Section 4.3 provides standard  
 357 membership inference attack and utility evaluations to contextualize our approach within existing  
 358 unlearning assessment practices.  
 359

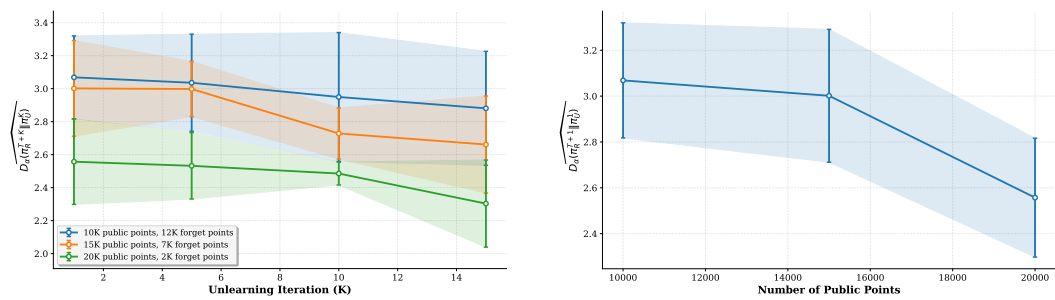
### 360 4.1 EVALUATING THE RÉNYI DIVERGENCE

361 **Experimental Setup.** We evaluate our approach on a multi-class image classification task using two  
 362 domains from the DomainNet dataset (Peng et al., 2019): Quickdraw (sketches) and Clipart (stylized  
 363 images), each containing 24 classes. We select these visually distinct domains to investigate how  
 364 public-private data alignment affects unlearning and performance (Fig. 4).

365 The experimental configuration treats Clipart images as private data (subject to unlearning) and  
 366 Quickdraw images as public data (permanently retained). For a training set of size  $n = n_{\text{pub}} + n_{\text{priv}}$ ,  
 367 we train models using cross-entropy loss and PNGD updates. To obtain samples from the weight  
 368 distributions  $\pi_U^K$  and  $\pi_R^T$ , we train  $N$  models in parallel: one set undergoes unlearning (fine-tuning  
 369 on the retain set after initial training), while another set trains from scratch on the retain set only.  
 370 This procedure yields  $N$  weight samples from each distribution, enabling empirical estimation of  
 371  $D_\alpha(\pi_U^K \parallel \pi_R^T)$  through the variational formulation (Theorem 4.1).  
 372

373 **Estimation Method.** We approximate the variational Rényi representation (Eq. (4)) using neural  
 374 network discriminators to parameterize the function space  $\mathcal{M}_b(\Omega)$ . This approach follows estab-  
 375 lished practices in divergence estimation (Birrell et al., 2021; 2023; Belghazi et al., 2021) (pseudo-  
 376 code in Appendix A.7.3). To reduce estimation variance, we apply spectral normalization (Miyato  
 377 et al., 2018) to regularize the discriminator networks. Complete details on discriminator architec-  
 378 ture and training procedures are provided in Appendix A.7. **Results.** Fig. 2a presents our Rényi

378 estimation results, demonstrating the effectiveness of public data injection for improving unlearning  
 379 efficiency. The experiments are conducted using  $N = 30,000$  models for each distribution and  
 380 averaged across 5 discriminator trainings with spectral normalization. The PGND noise scale is  
 381  $\sigma = 0.01$  and  $\alpha = 2$ . The results show that increasing public data volume reduces  $D_\alpha(\pi_R^{T+K} \parallel \pi_U^K)$ ,  
 382 with the divergence decreasing both as a function of unlearning iterations and public data proportion.  
 383 To understand the mechanism driving these improvements, we conduct an ablation study examining  
 384 the initial conditions after a *single* unlearning iteration. Fig. 2b isolates the effect of public data on  
 385 the starting distributions by measuring  $D_\alpha(\pi_R^{T+1} \parallel \pi_U^1)$  as a function of public data volume. Rather  
 386 than directly improving the unlearning procedure itself, public data creates more favorable initial  
 387 conditions by ensuring the learning and retraining weight distributions begin in closer proximity.  
 388 This mechanistic understanding validates our theoretical framework: public data primarily controls  
 389 the initial gap between distributions (Theorem 3.1), which then propagates through the unlearning  
 390 iterations to produce the final performance gains. Table 1 reports test accuracy for unlearned and  
 391 retrained models across different public/forget splits. Surprisingly, despite the public and private  
 392 data distributions being markedly different, the two procedures yield nearly identical accuracy (dif-  
 393 ferences  $\leq 0.05$ ). This observation indicates that the excess-risk bound in Proposition 3.3 can be  
 394 overly conservative. Hence, Langevin unlearning empirically achieves retraining-level generaliza-  
 395 tion even under unfavorable distribution shifts for this task. Identifying the structural conditions  
 396 under which this distributional term becomes negligible remains an important direction for future  
 397 work.



407 (a) Variational Rényi divergence estimation as a function  
 408 of public data proportion in the training set. The  
 409 results demonstrate that increasing public data volume  
 410 reduces  $D_\alpha(\pi_R^{T+K} \parallel \pi_U^K)$ , confirming improved  
 411 unlearning efficacy. This divergence also decreases  
 412 with the unlearning iterations.

407 (b) Ablation study: Initial distribution alignment as  
 408 a function of public data volume. The Rényi di-  
 409 vergence  $D_\alpha(\pi_R^{T+1} \parallel \pi_U^1)$  between retraining and un-  
 410 learning distributions after a single unlearning iteration  
 411 decreases as the number of public data points  
 412 increases.

413 Figure 2: Rényi divergence estimation for a different number of clipart images (public set)

## 416 4.2 DISTRIBUTION ALIGNMENT AND THE UNLEARNING-UTILITY TRADE-OFF

417 Theorem 3.3 characterizes a trade-off caused by public data volume: as we increase public data  
 418 volume, the *unlearning approximation error* decreases, yet the *distribution mismatch penalty* si-  
 419 multaneously grows. The balance between these competing terms determines whether public data  
 420 injection preserves or degrades model performance. To empirically investigate this trade-off, we  
 421 conduct experiments across two distinct distributional regimes: one where the public and private  
 422 domains exhibit moderate visual alignment, and another where they are substantially misaligned.

423 We fix  $K = 5$  unlearning iterations and evaluate performance using the DomainNet dataset across  
 424 two domain pairs. The **aligned regime** pairs Quickdraw (public) and Clipart (private), which despite  
 425 visual stylistic differences share semantic structure. The **misaligned regime** pairs Infograph (public)  
 426 and Real (private), which exhibit greater distributional divergence. We measure model performance  
 427 via loss on the private data distribution  $P_{\text{priv}}$  after unlearning, comparing against the retraining  
 428 baseline on the training mixture. Results are summarized in Table 1.

429 The results reveal a contrast between the two regimes. In the **aligned setting**, the relative perfor-  
 430 mance gap remains modest (3.68–4.62%) across varying public data volumes, suggesting that the  
 431 mismatch penalty remains manageable and the approximation error reduction dominates. In con-

432 Table 1: Unlearning vs Retraining Performance Across Distribution Alignments,  $K = 5$   
433

434 <b>Public</b>	435 <b>Private</b>	436 <b>Public</b>	437 <b>Private</b>	438 <b>Forget</b>	439 <b>Unlearn</b>	440 <b>Retrain</b>	441 <b>Rel.</b>
434 <b>Domain</b>	435 <b>Domain</b>	436 <b>Points</b>	437 <b>Points</b>	438 <b>Set</b>	439 <b>Avg. Loss</b>	440 <b>Avg. Loss</b>	441 <b>Diff (%)</b>
Quickdraw	Clipart	10000	20000	10000	3.102	2.976	4.23
Quickdraw	Clipart	30000	20000	10000	3.102	2.965	4.62
Quickdraw	Clipart	40000	20000	10000	3.099	2.989	3.68
Infograph	Real	10000	20000	10000	2.233	2.495	10.53
Infograph	Real	30000	20000	10000	2.238	2.496	10.34
Infograph	Real	40000	20000	10000	2.233	2.504	10.81

442  
443      trust, the **misaligned setting** exhibits a persistent performance gap (10.34–10.81%), with minimal  
444      sensitivity to public data volume. This indicates that when distributional divergence is large, increasing  
445      public data fails to overcome the mismatch penalty, rendering the approximation error reduction  
446      insufficient to improve generalization.  
447

### 448      4.3 PRACTICAL EVALUATION OF LU IN THE ASYMMETRIC SETTING

450      We now adopt standard evaluation methodology from the unlearning literature Hayes et al. (2024),  
451      introducing easily reproducible experiments which highlight that public data can benefit machine  
452      unlearning (LU). We provide an overview here and defer details to Appendix A.8.

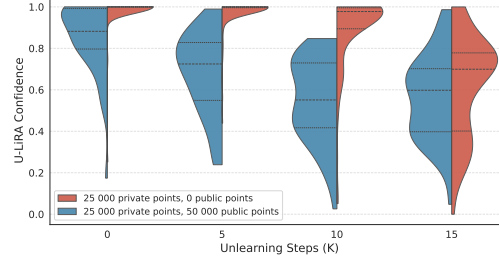
453      **Evaluation Method.** This evaluation is based on the U-LiRA membership inference attack for  
454      unlearning (Hayes et al., 2024; Carlini et al., 2021). Given a training set, forget set, and specified  
455      learning and unlearning algorithms, the adversary’s goal is to infer whether a model’s weights  $\theta$  were  
456      drawn from the unlearning distribution  $\pi_U^K$  or the retraining distribution  $\pi_R^{T+K}$ . Intuitively, lower  
457      attack accuracy indicates that the unlearning and retraining distributions are harder to distinguish,  
458      i.e., better unlearning.

459      In its most basic form, U-LiRA can be formalized via Bayes’ rule under a uniform prior on whether  
460      the forget set was included during training. Letting  $P(\theta | \cdot)$  denote the likelihood of observing  
461      model parameters  $\theta$  under a given distribution, and  $P(\cdot | \theta)$  as the posterior probability that  $\theta$  was  
462      drawn from that distribution, we have

$$463 \quad P(\pi_U^K | \theta) = \frac{P(\theta | \pi_U^K)}{P(\theta | \pi_U^K) + P(\theta | \pi_R^{T+K})}.$$

466      By selecting a one-dimensional representation of the models  $f : \Theta \rightarrow \mathbb{R}$  and as-  
467      suming that the induced distributions  $f_{\#}\pi_U^K$  and  $f_{\#}\pi_R^{T+K}$  are Gaussian, we can es-  
468      timate the likelihood terms  $P(\theta | \cdot)$  from a tractable number of model samples.  
469

470      **Experimental Setup.** For the sake of completeness, we focus this next set of experiments on a  
471      completely different task, namely sentiment analysis on the IMDB dataset of movie reviews (Maas  
472      et al., 2011). This is a simple binary classification  
473      task, where an LSTM (Hochreiter & Schmidhuber,  
474      1997) learns to recognize if a review is either  
475      negative or positive. We use the Amazon reviews  
476      dataset from Zhang et al. (2015) as the public data  
477      source. We use a forget set of 100 uniformly sam-  
478      pled examples from the IMDB dataset. For both  
479      experiments, i.e., with and without public data in-  
480      jection, we generate  $N = 50$  models to estimate  
481      each likelihood density, and report the empirical  
482      distribution of probabilities assigned to the right  
483      origin distribution by U-LiRA (confidence scores) for 50 models test (25 from  $\pi_U^K$ , and 25 from  
484       $\pi_R^{T+K}$ , where  $T = 50$  and  $K = 1 \rightarrow 15$ ). Fig. 3 highlights that without public data injection, U-  
485      LiRA is able to identify a large proportion of models confidently and correctly, even after a number  
486      of unlearning steps. This observed discriminative power is heavily impacted by public data injec-



487      Figure 3: U-LiRA confidence scores after  $K$  un-  
488      learning iterations as violin plots with quartiles.

489      490      491      492      493      494      495      496      497      498      499      500      501      502      503      504      505      506      507      508      509      510      511      512      513      514      515      516      517      518      519      520      521      522      523      524      525      526      527      528      529      530      531      532      533      534      535      536      537      538      539      540      541      542      543      544      545      546      547      548      549      550      551      552      553      554      555      556      557      558      559      560      561      562      563      564      565      566      567      568      569      570      571      572      573      574      575      576      577      578      579      580      581      582      583      584      585      586      587      588      589      590      591      592      593      594      595      596      597      598      599      600      601      602      603      604      605      606      607      608      609      610      611      612      613      614      615      616      617      618      619      620      621      622      623      624      625      626      627      628      629      630      631      632      633      634      635      636      637      638      639      640      641      642      643      644      645      646      647      648      649      650      651      652      653      654      655      656      657      658      659      660      661      662      663      664      665      666      667      668      669      670      671      672      673      674      675      676      677      678      679      680      681      682      683      684      685      686      687      688      689      690      691      692      693      694      695      696      697      698      699      700      701      702      703      704      705      706      707      708      709      710      711      712      713      714      715      716      717      718      719      720      721      722      723      724      725      726      727      728      729      730      731      732      733      734      735      736      737      738      739      740      741      742      743      744      745      746      747      748      749      750      751      752      753      754      755      756      757      758      759      760      761      762      763      764      765      766      767      768      769      770      771      772      773      774      775      776      777      778      779      780      781      782      783      784      785      786      787      788      789      790      791      792      793      794      795      796      797      798      799      800      801      802      803      804      805      806      807      808      809      810      811      812      813      814      815      816      817      818      819      820      821      822      823      824      825      826      827      828      829      830      831      832      833      834      835      836      837      838      839      840      841      842      843      844      845      846      847      848      849      850      851      852      853      854      855      856      857      858      859      860      861      862      863      864      865      866      867      868      869      870      871      872      873      874      875      876      877      878      879      880      881      882      883      884      885      886      887      888      889      890      891      892      893      894      895      896      897      898      899      900      901      902      903      904      905      906      907      908      909      910      911      912      913      914      915      916      917      918      919      920      921      922      923      924      925      926      927      928      929      930      931      932      933      934      935      936      937      938      939      940      941      942      943      944      945      946      947      948      949      950      951      952      953      954      955      956      957      958      959      960      961      962      963      964      965      966      967      968      969      970      971      972      973      974      975      976      977      978      979      980      981      982      983      984      985      986      987      988      989      990      991      992      993      994      995      996      997      998      999      9999

486  
487  
488  
489  
490  
491  
492  
493  
494  
495  
496  
497  
498  
499  
500  
501  
502  
503  
504  
505  
506  
507  
508  
509  
510  
511  
512  
513  
514  
515  
516  
517  
518  
519  
520  
521  
522  
523  
524  
525  
526  
527  
528  
529  
530  
531  
532  
533  
534  
535  
536  
537  
538  
539  
tion. We can also observe that modes of the confidence scores generally decrease with the number of unlearning steps, highlighting the unlearning effectiveness of LU.

Now that we've observed the effect of public data injection on the unlearning effectiveness of LU, we change our focus towards its impact on model utility. To this end, we report in Table 2 the average model accuracies over the 75 models we trained for each model distribution, on a test set of 10,000 unseen samples from the IMDB dataset. As the Amazon reviews dataset appears to be a good auxiliary public data source for the IMDB review classification problem (close data distributions), we also include an experiment in which a uniformly sampled 40% of its labels are flipped, thus increasing distribution mismatch between public and private sources.

Table 2: Unlearned and Retrained Model Test Accuracies for Different Scenarios

Private Dataset	Private Points	Public Dataset	Public Points	Flipped Public Labels	Unlearned Accuracy (%)	Retrained Accuracy (%)
IMDB	25,000	None	0	0%	82.59	82.54
		Amazon Reviews	50,000	0%	81.42	82.15
		Amazon Reviews	50,000	40%	80.40	80.80

From Table 2, we can observe that model accuracy does decrease from the injection of public data. However, this drop in accuracy is rather negligible compared to the extent to which public data injection improves the unlearning effectiveness of LU, which is highlighted by Fig. 3. As expected, the drop in accuracy is proportionately much lower when the quality of auxiliary public data is high (1.17% for unlearned and 0.39% for retrained) than when it is low (2.19% for unlearned, an  $\approx 1.87$  times increase, and 1.74% for retrained, an  $\approx 4.46$  times increase).

## 5 FUTURE WORK

Our analysis of Langevin unlearning with asymmetric data sources provides deeper insights into the unlearning-utility trade-off and raises interesting research questions, particularly regarding appropriate unlearning assumptions for different problem settings. A natural extension involves studying Langevin unlearning in fine-tuning contexts, where public data is learned prior to incorporating private data. We also propose developing adaptive unlearning algorithms that optimally balance data alignment with unlearning efficiency by leveraging techniques from domain adaptation and differential privacy. Another promising direction is a constrained optimization approach to asymmetric machine unlearning that extends beyond retain set fine-tuning, where the objective minimizes loss on the retain set subject to the constraint that the unlearning weight distribution remains sufficiently close to a distribution trained exclusively on public data.

From a theoretical perspective, existing Langevin unlearning analysis in both mini-batch and full batch settings (Chien et al., 2024a) still suffers from intractable log-Sobolev constants. Alternative isoperimetric assumptions (Chewi et al., 2021; Mousavi-Hosseini et al., 2023; Altschuler & Chewi, 2024) or adopting weaker divergence measures could yield more tractable bounds. While Rényi divergence provides natural connections to differential privacy, machine unlearning presents distinct challenges that may benefit from relaxed theoretical assumptions. Finally, extending our analysis from weight distributions to output distributions would facilitate both evaluation and analysis, while staying relevant for black-box commercial models.

## 6 CONCLUSION

We have studied Langevin unlearning under the assumption of asymmetric data sources, where datasets contain both private and public data. Our theoretical analysis demonstrates that this framework fundamentally improves the unlearning-utility trade-off by enabling control over unlearning guarantees through data supplementation rather than noise amplification. The framework provides fine-grained analysis of how distributional alignment between public and private data affects this trade-off: when distributions are well-aligned, public data injection preserves utility while maintaining unlearning guarantees, while misaligned distributions introduce controlled performance penalties that remain more manageable than traditional noise-based approaches.

540 7 REPRODUCIBILITY STATEMENT  
541

542 All theoretical results are supported by complete proofs in the Appendix (Theorems 3.1  
543 to 3.3 in Appendices A.1, A.3 and A.4, respectively). Our anonymized codebase, includ-  
544 ing experimental scripts and configurations, is available at <https://anonymous.4open.>  
545 [science/r/asymmetric\\_langevin\\_unlearning-34A3](https://anonymous.4open.) and <https://anonymous.>  
546 [4open.science/r/U-LiRAexperiments-EC08/">https://anonymous.4open.4open.science/r/U-LiRAexperiments-EC08/](https://anonymous.4open.). All experiments settings are detailed in  
547 Appendix A.7 and Appendix A.8

548  
549 REFERENCES  
550

551 Noga Alon, Raef Bassily, and Shay Moran. Limits of private learning with access to public data,  
552 2019a. URL <https://arxiv.org/abs/1910.11519>.

553 Noga Alon, Raef Bassily, and Shay Moran. Limits of Private Learning with Access to Public Data,  
554 2019b. *eprint*: 1910.11519.

555 Jason M. Altschuler and Sinho Chewi. Shifted Composition III: Local Error Framework  
556 for KL Divergence, December 2024. URL <http://arxiv.org/abs/2412.17997>.  
557 arXiv:2412.17997 [math].

558 Jason M Altschuler and Kunal Talwar. Resolving the mixing time of the langevin algorithm to its  
559 stationary distribution for log-concave sampling. *arXiv preprint arXiv:2210.08448*, 2022.

560 Ehsan Amid, Arun Ganesh, Rajiv Mathews, Swaroop Ramaswamy, Shuang Song, Thomas Steinke,  
561 Vinith M. Suriyakumar, Om Thakkar, and Abhradeep Thakurta. Public data-assisted mirror de-  
562 scent for private model training, 2022. URL <https://arxiv.org/abs/2112.00193>.

563 Idan Attias, Gintare Karolina Dziugaite, Mahdi Haghifam, Roi Livni, and Daniel M. Roy. Informa-  
564 tion Complexity of Stochastic Convex Optimization: Applications to Generalization, Memoriza-  
565 tion, and Tracing. In *Proceedings of the 41st International Conference on Machine Learning*,  
566 pp. 2035–2068. PMLR, July 2024. URL <https://proceedings.mlr.press/v235/attias24a.html>. ISSN: 2640-3498.

567 Mohamed Ishmael Belghazi, Aristide Baratin, Sai Rajeswar, Sherjil Ozair, Yoshua Bengio, Aaron  
568 Courville, and R. Devon Hjelm. MINE: Mutual Information Neural Estimation, August 2021.  
569 URL <http://arxiv.org/abs/1801.04062>. arXiv:1801.04062 [cs].

570 Jeremiah Birrell, Paul Dupuis, Markos A. Katsoulakis, Luc Rey-Bellet, and Jie Wang. Variational  
571 Representations and Neural Network Estimation of Rényi Divergences, July 2021. URL <http://arxiv.org/abs/2007.03814>. arXiv:2007.03814 [stat].

572 Jeremiah Birrell, Yannis Pantazis, Paul Dupuis, Markos A. Katsoulakis, and Luc Rey-Bellet.  
573 Function-space regularized Rényi divergences, February 2023. URL <http://arxiv.org/abs/2210.04974>. arXiv:2210.04974 [stat].

574 Lucas Bourtoule, Varun Chandrasekaran, Christopher A. Choquette-Choo, Hengrui Jia, Adelin  
575 Travers, Baiwu Zhang, David Lie, and Nicolas Papernot. Machine Unlearning, 2020. *eprint*:  
576 1912.03817.

577 Nicholas Carlini, Steve Chien, Milad Nasr, Shuang Song, A. Terzis, and Florian Tramèr. Member-  
578 ship inference attacks from first principles. *IEEE Symposium on Security and Privacy*, 2021. doi:  
579 10.1109/sp46214.2022.9833649.

580 Nicholas Carlini, Daphne Ippolito, Matthew Jagielski, Katherine Lee, Florian Tramer, and Chiyuan  
581 Zhang. Quantifying memorization across neural language models. In *The Eleventh International  
582 Conference on Learning Representations*, 2022.

583 Mathilde Caron, Hugo Touvron, Ishan Misra, Hervé Jégou, Julien Mairal, Piotr Bojanowski, and  
584 Armand Joulin. Emerging properties in self-supervised vision transformers, 2021. URL <https://arxiv.org/abs/2104.14294>.

594 Hong-Bin Chen, Sinho Chewi, and Jonathan Niles-Weed. Dimension-free log-sobolev inequalities  
 595 for mixture distributions. *Journal of Functional Analysis*, 281(11):109236, 2021.  
 596

597 Sinho Chewi. Log-concave sampling. *Book draft available at <https://chewisinho.github.io>*, 9:  
 598 17–18, 2023.

599 Sinho Chewi, Murat A. Erdogdu, Mufan Bill Li, Ruqi Shen, and Matthew Zhang. Analysis of  
 600 Langevin Monte Carlo from Poincaré to Log-Sobolev, December 2021. URL <http://arxiv.org/abs/2112.12662>. arXiv:2112.12662 version: 1.  
 601

602 Eli Chien, Haoyu Wang, Ziang Chen, and Pan Li. Langevin Unlearning: A New Perspective of  
 603 Noisy Gradient Descent for Machine Unlearning, 2024a. *eprint*: 2401.10371.  
 604

605 Eli Chien, Haoyu Wang, Ziang Chen, and Pan Li. Stochastic Gradient Langevin Unlearning, 2024b.  
 606 *eprint*: 2403.17105.  
 607

608 Rishav Chourasia, Jiayuan Ye, and Reza Shokri. Differential Privacy Dynamics of Langevin Diffu-  
 609 sion and Noisy Gradient Descent, February 2021. URL <https://arxiv.org/abs/2102.05855v5>.  
 610

611 Common Crawl Foundation. Common crawl: Open repository of web crawl data, 2024. URL  
 612 <https://commoncrawl.org/>. Multi-petabyte dataset containing over 100 billion web  
 613 pages.  
 614

615 Jia Deng, Wei Dong, Richard Socher, Li-Jia Li, Kai Li, and Li Fei-Fei. Imagenet: A large-scale hi-  
 616 erarchical image database. In *2009 IEEE conference on computer vision and pattern recognition*,  
 617 pp. 248–255. Ieee, 2009.

618 Monroe D Donsker and SR Srinivasa Varadhan. Asymptotic evaluation of certain markov process  
 619 expectations for large time, i. *Communications on pure and applied mathematics*, 28(1):1–47,  
 620 1975.

621 Tim van Erven and Peter Harremoës. Rényi Divergence and Kullback-Leibler Divergence. *IEEE  
 622 Transactions on Information Theory*, 60(7):3797–3820, July 2014. ISSN 0018-9448, 1557-  
 623 9654. doi: 10.1109/TIT.2014.2320500. URL <http://arxiv.org/abs/1206.2459>.  
 624 arXiv:1206.2459 [cs].  
 625

626 Arun Ganesh, Mahdi Haghifam, Milad Nasr, Sewoong Oh, Thomas Steinke, Om Thakkar,  
 627 Abhradeep Guha Thakurta, and Lun Wang. Why is public pretraining necessary for private  
 628 model training? In Andreas Krause, Emma Brunskill, Kyunghyun Cho, Barbara Engelhardt,  
 629 Sivan Sabato, and Jonathan Scarlett (eds.), *Proceedings of the 40th International Conference  
 630 on Machine Learning*, volume 202 of *Proceedings of Machine Learning Research*, pp. 10611–  
 631 10627. PMLR, 23–29 Jul 2023a. URL <https://proceedings.mlr.press/v202/ganesh23a.html>.  
 632

633 Arun Ganesh, Mahdi Haghifam, Milad Nasr, Sewoong Oh, Thomas Steinke, Om Thakkar,  
 634 Abhradeep Thakurta, and Lun Wang. Why Is Public Pretraining Necessary for Private Model  
 635 Training?, 2023b. URL <https://arxiv.org/abs/2302.09483>. *eprint*: 2302.09483.  
 636

637 Alison L. Gibbs and Francis Edward Su. On choosing and bounding probability metrics, September  
 638 2002. URL <http://arxiv.org/abs/math/0209021>. arXiv:math/0209021.  
 639

640 Aditya Golatkar, Alessandro Achille, and Stefano Soatto. Eternal Sunshine of the Spotless Net:  
 641 Selective Forgetting in Deep Networks, 2020. URL <https://arxiv.org/abs/1911.04933>.  
 642 *eprint*: 1911.04933.

643 Aditya Golatkar, Alessandro Achille, Avinash Ravichandran, Marzia Polito, and Stefano Soatto.  
 644 Mixed-Privacy Forgetting in Deep Networks, 2021. URL <https://arxiv.org/abs/2012.13431>.  
 645 *eprint*: 2012.13431.

646 Thomas Hakon Gronwall. Note on the derivatives with respect to a parameter of the solutions of a  
 647 system of differential equations. *Annals of Mathematics*, 20(4):292–296, 1919.

648 Leonard Gross. Logarithmic sobolev inequalities. *American Journal of Mathematics*, 97(4):1061–  
 649 1083, 1975.

650

651 Moritz Hardt, Ben Recht, and Yoram Singer. Train faster, generalize better: Stability of stochastic  
 652 gradient descent. In *International conference on machine learning*, pp. 1225–1234. PMLR, 2016.

653

654 Jamie Hayes, Ilia Shumailov, Eleni Triantafillou, Amr Khalifa, and Nicolas Papernot. Inexact Un-  
 655 learning Needs More Careful Evaluations to Avoid a False Sense of Privacy, May 2024. URL  
 656 <http://arxiv.org/abs/2403.01218>. arXiv:2403.01218 [cs].

657

658 Jamie Hayes, Ilia Shumailov, Eleni Triantafillou, Amr Khalifa, and Nicolas Papernot. Inexact Un-  
 659 learning needs more careful evaluations to avoid a false sense of privacy. In *2025 IEEE Conference on Secure and Trustworthy Machine Learning (SaTML)*, pp. 497–519, 2025. doi:  
 660 10.1109/SaTML64287.2025.00034.

661

662 Sepp Hochreiter and Jürgen Schmidhuber. Long short-term memory. *Neural Computation*, 9(8):  
 663 1735–1780, 1997. doi: 10.1162/neco.1997.9.8.1735.

664

665 Diederik P. Kingma and Jimmy Ba. Adam: A method for stochastic optimization, 2017. URL  
 666 <https://arxiv.org/abs/1412.6980>.

667

668 Anastasia Koloskova, Youssef Allouah, Animesh Jha, Rachid Guerraoui, and Sanmi Koyejo. Cer-  
 669 tified Unlearning for Neural Networks, June 2025. URL <http://arxiv.org/abs/2506.06985>. arXiv:2506.06985 [cs].

670

671 Andrew G. Lamperski. Projected Stochastic Gradient Langevin Algo-  
 672 rithms for Constrained Sampling and Non-Convex Learning. *ArXiv*, De-  
 673 cember 2020. URL <https://www.semanticscholar.org/paper/ede5a9ae87c1dee98098c243f6b44c30804acbdf>.

674

675 Andrew Lowy, Zeman Li, Tianjian Huang, and Meisam Razaviyayn. Optimal differentially private  
 676 model training with public data. In *Proceedings of the 41st International Conference on Machine  
 677 Learning*, ICML’24. JMLR.org, 2024.

678

679 Andrew L. Maas, Raymond E. Daly, Peter T. Pham, Dan Huang, Andrew Y. Ng, and Christopher  
 680 Potts. Learning word vectors for sentiment analysis. In *Proceedings of the 49th Annual Meeting  
 681 of the Association for Computational Linguistics: Human Language Technologies*, pp. 142–150,  
 682 Portland, Oregon, USA, June 2011. Association for Computational Linguistics. URL <http://www.aclweb.org/anthology/P11-1015>.

683

684 Ilya Mironov. Renyi Differential Privacy. In *2017 IEEE 30th Computer Security Foundations  
 685 Symposium (CSF)*, pp. 263–275, August 2017. doi: 10.1109/CSF.2017.11. URL <http://arxiv.org/abs/1702.07476>. arXiv:1702.07476 [cs].

686

687 Takeru Miyato, Toshiki Kataoka, Masanori Koyama, and Yuichi Yoshida. Spectral Normalization for  
 688 Generative Adversarial Networks, February 2018. URL <http://arxiv.org/abs/1802.05957>. arXiv:1802.05957 [cs].

689

690 Alireza Mousavi-Hosseini, Tyler K. Farghly, Ye He, Krishna Balasubramanian, and Murat A. Er-  
 691 dogdu. Towards a complete analysis of langevin monte carlo: Beyond poincaré inequality.  
 692 In *The Thirty Sixth Annual Conference on Learning Theory*, pp. 1–35. PMLR, 2023. URL  
 693 <https://proceedings.mlr.press/v195/mousavi-hosseini23a.html>.

694

695 Milad Nasr, Nicholas Carlini, Jonathan Hayase, Matthew Jagielski, A Feder Cooper, Daphne Ip-  
 696 polito, Christopher A Choquette-Choo, Eric Wallace, Florian Tramèr, and Katherine Lee. Scalable  
 697 extraction of training data from (production) language models. *arXiv preprint arXiv:2311.17035*,  
 698 2023.

699

700 Jerzy Neyman and Egon Sharpe Pearson. Ix. on the problem of the most efficient tests of statistical  
 701 hypotheses. *Philosophical Transactions of the Royal Society of London. Series A, Containing  
 Papers of a Mathematical or Physical Character*, 231(694-706):289–337, 1933.

702 Maxime Oquab, Timothée Darcet, Théo Moutakanni, Huy Vo, Marc Szafraniec, Vasil Khalidov,  
 703 Pierre Fernandez, Daniel Haziza, Francisco Massa, Alaaeldin El-Nouby, Mahmoud Assran, Nico-  
 704 las Ballas, Wojciech Galuba, Russell Howes, Po-Yao Huang, Shang-Wen Li, Ishan Misra, Michael  
 705 Rabbat, Vasu Sharma, Gabriel Synnaeve, Hu Xu, Hervé Jegou, Julien Mairal, Patrick Labatut, Ar-  
 706 mand Joulin, and Piotr Bojanowski. Dinov2: Learning robust visual features without supervision,  
 707 2024. URL <https://arxiv.org/abs/2304.07193>.

708 European Parliament and Council of the European Union. Regulation (eu) 2024/1689 of the eu-  
 709 ropean parliament and of the council of 13 june 2024 laying down harmonised rules on artificial  
 710 intelligence and amending regulations (ec) no 300/2008, (eu) no 167/2013, (eu) no 168/2013, (eu)  
 711 2018/858, (eu) 2018/1139 and (eu) 2019/2144 and directives 2014/90/eu, (eu) 2016/797 and (eu)  
 712 2016/798 (artificial intelligence act). Official Journal of the European Union, July 2024. URL  
 713 <https://eur-lex.europa.eu/eli/reg/2024/1689/oj/eng>. Entered into force:  
 714 1 August 2024.

715 Parliament of Canada. An act to enact the consumer privacy protection act, the personal information  
 716 and data protection tribunal act and the artificial intelligence and data act and to make conse-  
 717 quential and related amendments to other acts. Bill C-27, 44th Parliament, 1st Session, 2022.  
 718 URL <https://www.parl.ca/legisinfo/en/bill/44-1/c-27>. Digital Charter Im-  
 719 plementation Act, 2022.

720 Xingchao Peng, Qinxun Bai, Xide Xia, Zijun Huang, Kate Saenko, and Bo Wang. Moment matching  
 721 for multi-source domain adaptation. In *Proceedings of the IEEE International Conference on*  
 722 *Computer Vision*, pp. 1406–1415, 2019.

723 Maxim Raginsky, Alexander Rakhlin, and Matus Telgarsky. Non-convex learning via Stochastic  
 724 Gradient Langevin Dynamics: a nonasymptotic analysis, 2017. URL <https://arxiv.org/abs/1702.03849>. eprint: 1702.03849.

725 Reza Shokri, Marco Stronati, Congzheng Song, and Vitaly Shmatikov. Membership inference  
 726 attacks against machine learning models, 2017. URL <https://arxiv.org/abs/1610.05820>.

727 Santosh Vempala and Andre Wibisono. Rapid Convergence of the Unadjusted Langevin Algorithm:  
 728 Isoperimetry Suffices. In H. Wallach, H. Larochelle, A. Beygelzimer, F. d' Alché-Buc, E. Fox,  
 729 and R. Garnett (eds.), *Advances in Neural Information Processing Systems*, volume 32. Cur-  
 730 ran Associates, Inc., 2019. URL [https://proceedings.neurips.cc/paper\\_files/paper/2019/file/65a99bb7a3115fdede20da98b08a370f-Paper.pdf](https://proceedings.neurips.cc/paper_files/paper/2019/file/65a99bb7a3115fdede20da98b08a370f-Paper.pdf).

731 Cédric Villani et al. *Optimal transport: old and new*, volume 338. Springer, 2009.

732 Pan Xu, Jinghui Chen, Difan Zou, and Quanquan Gu. Global convergence of langevin dynam-  
 733 ics based algorithms for nonconvex optimization. *Advances in Neural Information Processing*  
 734 *Systems*, 31, 2018.

735 Haonan Yan, Xiaoguang Li, Ziyao Guo, Hui Li, Fenghua Li, and Xiaodong Lin. ARCANe: An  
 736 Efficient Architecture for Exact Machine Unlearning. volume 5, pp. 4006–4013, July 2022. doi:  
 737 10.24963/ijcai.2022/556. URL <https://www.ijcai.org/proceedings/2022/556>.  
 ISSN: 1045-0823.

738 Jiayuan Ye and Reza Shokri. Differentially Private Learning Needs Hidden State (Or Much Faster  
 739 Convergence), March 2022. URL <https://arxiv.org/abs/2203.05363v2>.

740 Chiyuan Zhang, Samy Bengio, Moritz Hardt, Benjamin Recht, and Oriol Vinyals. Understanding  
 741 deep learning requires rethinking generalization. *arXiv preprint arXiv:1611.03530*, 2016.

742 Xiang Zhang, Junbo Zhao, and Yann LeCun. Character-level convolutional networks for text classi-  
 743 fication. In *Proceedings of the 29th International Conference on Neural Information Processing*  
 744 *Systems - Volume 1*, NIPS'15, pp. 649–657, Cambridge, MA, USA, 2015. MIT Press.

756 **A APPENDIX**  
 757

758 **A.1 PROOF OF THEOREM 3.2**  
 759

760 **Theorem.** (Chien et al., 2024a) Suppose that the loss is  $L$ -smooth and  $M$ -Lipschitz, and that the  
 761 learning distribution of weights at time  $T$  satisfies a  $C$  log-Sobolev inequality. Then, the Rényi di-  
 762 vergence between  $\pi_U^K$  (the unlearning distribution after  $K$  iterations) and the retraining distribution  
 763 after  $T + K$  iterations is upper bounded by:

764 
$$D_\alpha(\pi_R^{T+K} \| \pi_U^K) \leq D_\alpha(\pi_L^T \| \pi_R^T) \exp\left(-\frac{1}{\alpha} \sum_{k=0}^{K-1} R_k\right)$$
  
 765  
 766

767 where  $R_k > 0$  depend on the problem setting (Chien et al., 2024a). Moreover, if the loss function  
 768 is  $m$ -strongly convex and the initial log-Sobolev constant satisfies  $C > \frac{\sigma^2}{m}$ , we get the following  
 769 exponential decay of the Rényi divergence with respect to the unlearning iteration:  
 770

771 
$$D_\alpha(\pi_R^{T+K} \| \pi_U^K) \leq D_\alpha(\pi_L^T \| \pi_R^T) \exp\left(-\frac{2K\sigma^2\eta}{C\alpha}\right)$$
  
 772  
 773

774 We provide the proof of (Chien et al., 2024a), Theorem 3.2, slightly modified to our setting. Specif-  
 775 ically, we relax the assumption that the learning and retraining processes have converged to their  
 776 stationary distribution (infinite training). In order to prove this theorem, we will use the following  
 777 lemmas:

778 **Lemma A.1** (Characterizing the log-Sobolev constants of the PNGD updates (Chewi, 2023)). Con-  
 779 sider the PNGD update:  
 780

781 
$$\theta^{k+1} = \Pi_\Theta \left[ \theta_k - \eta \nabla \mathcal{L}_D(\theta^k) + \sqrt{2\eta\sigma^2} W_k \right], \theta^0 \sim \pi$$
  
 782

783 where  $\pi$  satisfies a  $C$ -Log Sobolev inequality. Then, we have the following:  
 784

- 785 • If  $\mathcal{L}$  is  $L$ -smooth, then for the gradient update  $h(\theta) = \theta - \nabla_\theta \mathcal{L}(\theta)$ , we have that the  
 786 distribution of  $h_\sharp \pi$  satisfies a  $(1 + \eta L)^2 \times C$  log-Sobolev inequality. Moreover, if  $\mathcal{L}$  is  
 787  $m$ -strongly convex and  $\eta < \frac{1}{L}$ , then  $h_\sharp \pi$  satisfies a  $(1 - \eta m)^2 \times C$  log Sobolev inequality  
 788 (Altschuler & Talwar, 2022).
- 789 •  $\pi * \mathcal{N}(0, \sigma^2 I_d)$  satisfies a  $C + \sigma^2$  log-Sobolev inequality
- 790 •  $\Pi_{\Theta \sharp} \pi$  satisfies a  $C$  log-Sobolev inequality

793 By composing the aforementioned statements, we get that  $\pi_1$  satisfies a  $(1 + \eta L)^2 \times C + 2\eta\sigma^2$ -log  
 794 Sobolev inequality. Moreover, if  $\mathcal{L}$  is  $m$ -strongly convex and  $\eta < \frac{1}{L}$ , we have that  $\pi_1$  satisfies a  
 795  $(1 - \eta m)^2 \times C + 2\eta\sigma^2$

796 **Lemma A.2** (Data Processing inequality for the Rényi divergence (Erven & Harremoës, 2014)). For  
 797 any  $\alpha \geq 1$ , any function  $h : \mathbb{R}^d \rightarrow \mathbb{R}^d$  and distributions  $P, Q$  supported on  $\mathbb{R}^d$ , we have:  
 798

799 
$$D_\alpha(h_\sharp P \| h_\sharp Q) \leq D_\alpha(P \| Q)$$

800 with equality if  $h$  is bijective

801 **Lemma A.3** ((Vempala & Wibisono, 2019; Chien et al., 2024a) characterizing the Rényi divergence  
 802 between two distributions convoluted with Gaussians). Let  $P_t = P * \mathcal{N}(0, 2t\sigma^2 I_d)$  and  $Q_t =$   
 803  $Q * \mathcal{N}(0, 2t\sigma^2 I_d)$ . Then,  $\forall \alpha > 0$ :

804 
$$\frac{\partial D_\alpha(P_t \| Q_t)}{\partial t} = -\alpha \sigma^2 \frac{G_\alpha(P_t \| Q_t)}{F_\alpha(P_t \| Q_t)}$$
  
 805  
 806

807 with  $G_\alpha(P \| Q) = \mathbb{E}_Q \left[ \left( \frac{p}{q} \right)^\alpha \| \nabla \log \frac{p}{q} \|^2 \right]$  denoting the relative Rényi information and  $F_\alpha(P \| Q) =$   
 808  $\mathbb{E}_Q \left[ \left( \frac{p}{q} \right)^\alpha \right] = \exp((\alpha - 1)D_\alpha(P \| Q))$   
 809

810  
 811 **Lemma A.4.** *Lower bound of the G-F ratio (Vempala & Wibisono, 2019)* If  $Q \in \mathcal{P}(\Theta)$  satisfies a  
 812  $C \log$  Sobolev inequality, then  $\forall P \in \mathcal{P}(\Theta)$ :

$$\frac{G_\alpha(P\|Q)}{F_\alpha(P\|Q)} \geq \frac{2D_\alpha(P\|Q)}{\alpha^2 C}$$

813 **Lemma A.5.** *Grönwall's inequality (Gronwall, 1919)* Let  $\mathbf{I} = [a, b]$  denote an interval on the real  
 814 line. Let  $\beta$  and  $u$  be real-valued continuous functions defined on  $\mathbf{I}$ . If  $u$  is differentiable in the  
 815 interior of  $\mathbf{I}$  and satisfies for all  $t$  in the interior of  $\mathbf{I}$ :

$$\frac{du(t)}{dt} \leq \beta(t)u(t)$$

816 then we have:

$$u(t) \leq u(a) \exp \left( \int_a^t \beta(s) ds \right)$$

817 for all  $t \in I$

818 **Lemma A.6.** *Universal upper bound on the log Sobolev constant for measures with compact support*  
 819 (Chen et al., 2021) Let  $P$  a probability measure supported on a compact set with radius  $R$ . Then,  
 820 for each  $\sigma > 0$ ,  $P * \mathcal{N}(0, \sigma I_d)$  satisfy a log Sobolev inequality with constant upper bounded by  
 821  $6(4R^2 + \sigma) \exp \left( \frac{4R^2}{\sigma} \right)$

822 *Proof.* Using these results, we have:

$$D_\alpha(h_\# \pi_R^{T+K} \| h_\# \pi_U^K) \leq D_\alpha(\pi_R^{T+K} \| \pi_U^K) \quad (\text{Lemma A.2})$$

823 **The PNGD updates preserve the log-Sobolev inequality for the resulting distributions:** let  
 824  $\pi_U^{K,1,t} = h_\# \pi_U^K * \mathcal{N}(0, 2t\sigma^2 I_d)$  and  $\pi_R^{T+K,1,t} = h_\# \pi_U^K * \mathcal{N}(0, 2t\sigma^2 I_d)$ . Since  $\pi_L^T$  and  $\pi_R^T$  sat-  
 825 isfy a log-Sobolev inequality (initialization distributions) and the loss function is  $L$ -smooth, then by  
 826 Lemma A.1 the distributions  $\pi_U^K, \pi_L^T$  satisfy respectively  $C_{U,K}, C_{L,T+K}$  log Sobolev inequal-  
 827 ities. Using Lemma A.1 on the distributions  $\pi_U^{K,1,t}, \pi_R^{T+K,1,t}$  yields that they respectively satisfy  
 828  $(1 + \eta L)^2 C_{U,K} + 2\eta\sigma^2$  and  $(1 + \eta L)^2 C_{L,T+K} + 2\eta\sigma^2$  log Sobolev inequalities for all  $t \in [0, \eta]$ .

829 **Upper bounding the distributions convolved with Gaussian distributions:** Using Lemma A.3,  
 830 we have that,  $\forall \alpha > 0$ :

$$\frac{\partial D_\alpha(\pi_R^{T+K,1,t} \| \pi_U^{K,1,t})}{\partial t} = -\alpha\sigma^2 \frac{G_\alpha(\pi_R^{T+K,1,t} \| \pi_U^{K,1,t})}{F_\alpha(\pi_R^{T+K,1,t} \| \pi_U^{K,1,t})}$$

831 and since  $\pi_U^{K,1,t}$  satisfies a  $C_{U,K,t} = (1 + \eta L)^2 C_{U,K} + 2t\sigma^2$  log-Sobolev inequality, we can use  
 832 Lemma A.4 to upper bound the derivative of the Rényi divergence with respect to  $t \in [0, \eta]$ :

$$\frac{\partial D_\alpha(\pi_R^{T+K,1,t} \| \pi_U^{K,1,t})}{\partial t} \leq -\frac{2\sigma^2}{\alpha C_{U,K,t}} D_\alpha(\pi_R^{T+K,1,t} \| \pi_U^{K,1,t})$$

833 Thus, by Grönwall's inequality (Lemma A.5), we have  $\forall t \in [0, \eta]$ :

$$\begin{aligned} D_\alpha(\pi_R^{T+K,1,t} \| \pi_U^{K,1,t}) &\leq D_\alpha(h_\# \pi_R^{T+K} \| h_\# \pi_U^K) \exp \left( \int_0^t -\frac{2\sigma^2}{\alpha C_{U,K,s}} ds \right) \\ &\leq D_\alpha(h_\# \pi_R^{T+K} \| h_\# \pi_U^K) \exp \left( \int_0^t -\frac{2\sigma^2}{\alpha ((1 + \eta L)^2 C_{U,K} + 2s\sigma^2)} ds \right) \\ &\leq D_\alpha(\pi_R^{T+K} \| \pi_U^K) \exp \left( \int_0^t -\frac{2\sigma^2}{\alpha ((1 + \eta L)^2 C_{U,K} + 2s\sigma^2)} ds \right) \end{aligned} \quad (\text{Lemma A.2})$$

834 Computing the integral yields:

$$\begin{aligned} \int_0^t -\frac{2\sigma^2}{\alpha ((1 + \eta L)^2 C_{U,K} + 2s\sigma^2)} ds &= -\frac{1}{\alpha} \int_0^t \frac{2\sigma^2}{(1 + \eta L)^2 C_{U,K} + 2s\sigma^2} ds \\ &= -\frac{1}{\alpha} \left[ \log ((1 + \eta L)^2 C_{U,K} + 2t\sigma^2) - \log ((1 + \eta L)^2 C_{U,K}) \right] \\ &= -\frac{1}{\alpha} \left[ \log \left( 1 + \frac{2t\sigma^2}{(1 + \eta L)^2 C_{U,K}} \right) \right] \end{aligned}$$

864 Thus, by setting  $t = \eta$ , we get:  
 865

$$866 \quad D_\alpha(\pi_R^{T+K,1,\eta} \|\pi_U^{K,1,\eta}) \leq \left(1 + \frac{2t\sigma^2}{(1+\eta L)^2 C_{U,K}}\right)^{\frac{-1}{\alpha}} D_\alpha(\pi_R^{T+K} \|\pi_U^K)$$

$$867$$

$$868$$

869 Finally, using the data processing inequality for the projection of PNGD and iterating over the num-  
 870 ber of unlearning iterations, we get:  
 871

$$872 \quad D_\alpha(\pi_R^{T+K+1} \|\pi_U^{K+1}) \leq D_\alpha(\pi_R^{T+K,1,\eta} \|\pi_U^{K,1,\eta})$$

$$873$$

$$874 \quad \leq \left(1 + \frac{2t\sigma^2}{(1+\eta L)^2 C_{U,K}}\right)^{\frac{-1}{\alpha}} D_\alpha(\pi_R^{T+K} \|\pi_U^K)$$

$$875$$

$$876 \quad \leq D_\alpha(\pi_R^T \|\pi_L^T) \prod_{k=1}^K \left(1 + \frac{2t\sigma^2}{(1+\eta L)^2 C_{U,k}}\right)^{\frac{-1}{\alpha}}$$

$$877$$

$$878$$

□

## 881 A.2 TRACKING THE LOG-SOBOLEV CONSTANTS

882 For a generic,  $L$ -smooth non-convex loss function  $\mathcal{L}$ , one can derive the following recurrence rela-  
 883 tion,  $\forall k \geq 1$  upper bounding the log-Sobolev constants:  
 884

$$885 \quad C_1 \leq (1+\eta L)^2 C_0 + 2\eta\sigma^2 \quad (\text{Lemma A.1})$$

$$886$$

$$887 \quad C_2 \leq (1+\eta L)^4 C_0 + (1+\eta L)^2 2\eta\sigma^2 + (1+\eta L)^2$$

$$888 \quad \dots$$

$$889$$

$$890 \quad C_K \leq (1+\eta L)^{2K} C_0 + 2\eta\sigma^2 \sum_{k=0}^{K-1} (1+\eta L)^2$$

$$891$$

$$892 \quad \leq (1+\eta L)^{2K} C_0 + 2\eta\sigma^2 \frac{(1+\eta L)^{2K} - 1}{(1+\eta L)^2 - 1} \quad (5)$$

$$893$$

$$894$$

895 If we add the assumption that the loss is convex, then the map  $h(\theta) = \theta - \eta \nabla_\theta \mathcal{L}(\theta)$  is 1-Lipschitz  
 896 for  $\eta < \frac{2}{L}$  (Hardt et al., 2016) and we can reduce  $(1+\eta L)$  to 1 in the aforementioned bounds:  
 897

$$898 \quad C_K \leq C_0 + 2K\eta\sigma^2 \quad (6)$$

$$899$$

900 Finally, assuming  $m$ -strong convexity yields that the map  $h(\theta)$  is  $1 - \eta m$ -Lipschitz, which allows  
 901 for the following **contractive** recurrence on the log-Sobolev constants  $\forall k \geq 1$  by setting  $\eta <$   
 902  $\frac{2}{m}(1 - \frac{\sigma^2}{mC_0})$  (Chien et al., 2024a):  
 903

$$904 \quad C_k \leq (1 - \eta m)^2 C_{k-1} + 2\eta\sigma^2 \leq C_{k-1}$$

$$905 \quad C_k \leq (1 - \eta m)^{2K} C_0 + 2\eta\sigma^2 \frac{(1 - \eta m)^{2K} - 1}{(1 - \eta m)^2 - 1} \leq C_0$$

$$906$$

907 Thus, we have that  $\forall t \in [0, \eta]$ ,  $\pi_U^{K,1,t}$  satisfies a  $C_0$  log-Sobolev inequality thus we have by  
 908 Lemma A.4:  
 909

$$910 \quad \frac{\partial D_\alpha(\pi_R^{T+K,1,t} \|\pi_U^{K,1,t})}{\partial t} \leq -\frac{2\sigma^2}{\alpha C} D_\alpha(\pi_R^{T+K,1,t} \|\pi_U^{K,1,t})$$

$$911$$

912 Thus, by Grönwall's inequality (Lemma A.5), we have  $\forall t \in [0, \eta]$ :  
 913

$$914 \quad \frac{\partial D_\alpha(\pi_R^{T+K,1,t} \|\pi_U^{K,1,t})}{\partial t} \leq D_\alpha(h_\sharp \pi_R^{T+K} \| h_\sharp \pi_U^K) \exp\left(\int_0^t -\frac{2\sigma^2}{\alpha C} ds\right)$$

$$915$$

$$916 \quad \leq D_\alpha(h_\sharp \pi_R^{T+K} \| h_\sharp \pi_U^K) \exp\left(-\frac{2t\sigma^2}{\alpha C}\right)$$

$$917$$

918 Thus, by setting  $t = \eta$  and using similar steps as the non convex proof above, we get the following  
 919 result:

$$920 \quad 921 \quad 922 \quad D_\alpha(\pi_R^{T+K} \|\pi_U^K) \leq D_\alpha(\pi_R^T \|\pi_L^T) \exp\left(-\frac{2K\eta\sigma^2}{\alpha C}\right)$$

923 The message conveyed by the strongly convex proof is that if we have a universal iteration inde-  
 924 pendent upper bound on the log Sobolev constants at each timestep of the PNGD updates, then we  
 925 could have a more meaningful upper bound on the Rényi divergence. The non convex Eq. (5) and  
 926 convex Eq. (6) recurrence bounds are non contractive and iteration dependent, so they do not allow  
 927 to establish a convergence rate for Theorem 3.2. This is where the projection step of PNGD comes  
 928 in handy, as it allows to leverage the geometry of the set  $\Theta$  to get a more informative bound:

929 **Lemma A.7** (Log Sobolev inequality on measures supported on a compact set (Chen et al., 2021),  
 930 Corollary 1). *Let  $\pi$  be a probability measure on  $\mathbb{R}^d$  supported on a compact set  $\Theta$  with radius  
 931  $R \geq 0$ . Then, for each  $t \geq 0$ ,  $\mu * \mathcal{N}(0, tI_d)$  satisfy a log sobolev inequality with constant  $C$   
 932 controlled by:*

$$933 \quad 934 \quad C \leq 6(4R^2 + t) \exp\left(\frac{4R^2}{t}\right)$$

935 **Proposition A.1** (Universal bound on the log Sobolev constants of distributions induced by PNGD  
 936 updates (Chien et al., 2024a)). *Suppose that  $\mathcal{L}$  is  $M$  Lipschitz. Let  $\theta_0 \sim \pi_0 \in \mathcal{P}(\Theta)$  where  $\Theta$  is a  
 937 compact set of radius  $R$  and denote by  $\pi_k$  the distribution  $\theta_k$ , the  $k$ -th iterate of PNGD (Eq. (2)).  
 938 Then,  $\forall k \geq 0$ ,  $\pi_k$  satisfies a log-Sobolev inequality with constant  $C_k$  controlled by:*

$$939 \quad 940 \quad C_k \leq 6(4(R + \eta M)^2 + 2\eta\sigma^2) \exp\left(\frac{4(R + \eta M)^2}{2\eta\sigma^2}\right)$$

941 We can thus derive a similar bound to the strongly convex setting, for the non convex/convex  
 942 settings:

943 Using Proposition A.1, we have  $\forall k \geq 0$  that  $\pi_U^K$  satisfies a  $\tilde{C} =$   
 944  $6(4(R + \eta M)^2 + 2\eta\sigma^2) \exp\left(\frac{4(R + \eta M)^2}{2\eta\sigma^2}\right)$  log Sobolev inequality. Thus, using Lemma A.4,  
 945 we have:

$$946 \quad \frac{\partial D_\alpha(\pi_R^{T+K,1,t} \|\pi_U^{K,1,t})}{\partial t} \leq -\frac{2\sigma^2}{\alpha\tilde{C}} D_\alpha(\pi_R^{T+K,1,t} \|\pi_U^{K,1,t})$$

947 Thus, by Grönwall's inequality (Lemma A.5), we have  $\forall t \in [0, \eta]$ :

$$948 \quad 949 \quad \frac{\partial D_\alpha(\pi_R^{T+K,1,t} \|\pi_U^{K,1,t})}{\partial t} \leq D_\alpha(h_\sharp \pi_R^{T+K} \|\pi_U^K) \exp\left(\int_0^t -\frac{2\sigma^2}{\alpha\tilde{C}} ds\right)$$

$$950 \quad 951 \quad \leq D_\alpha(h_\sharp \pi_R^{T+K} \|\pi_U^K) \exp\left(-\frac{2t\sigma^2}{\alpha\tilde{C}}\right)$$

952 Finally, similarly to the strongly convex proofs, we can deduce that:

$$953 \quad 954 \quad D_\alpha(\pi_R^{T+K} \|\pi_U^K) \leq D_\alpha(\pi_R^T \|\pi_L^T) \exp\left(-\frac{2K\eta\sigma^2}{\alpha\tilde{C}}\right)$$

### 955 A.3 PROOF OF THEOREM 3.1

956 **Theorem.** *Suppose that the loss is  $L$ -smooth and  $M$ -Lipschitz, and that the initialization distribu-  
 957 tion satsfies a  $C$ -log Sobolev inequality. Moreover, suppose that the PNGD updates project onto a  
 958 compact set  $\Theta$  of radius  $R$ .*

959 *Then at learning iteration  $T$ , we have the following upper bound on the Renyi divergence between  
 960 the retraining  $\pi_R^T$  and learning  $\pi_L^T$  distributions:*

$$961 \quad 962 \quad 963 \quad \frac{D_\alpha(\pi_R^T \|\pi_L^T)}{\alpha} \leq \frac{2M^2\eta^2 n_{\text{forget}}^2}{(n_{\text{pub}} + n_{\text{priv}})^2 \sigma^2} \sum_{t=1}^{T-1} \prod_{t'=t}^{T-1} \left(1 + \frac{\eta\sigma^2}{C_{t',1}}\right)^{-1}$$

964 where  $C_{t',1} > 0$  are log Sobolev constants of the distributions of the intermediate PNGD updates.  
 965 Using the support's radius allows to loosely upper bound those constants (Chien et al., 2024a):  
 966  $C_{t',1} \leq 6e^{4\tau}(4\tau^2 + \eta\sigma^2)$  with  $\tau = R + \eta M$

972 *Proof.* The following proof is an adaptation of the proof of Theorem 3.2 in Chien et al. (2024a) to  
 973 the asymmetric data setting.

974 Consider the following updates done during training. Recall that we are using full batch projected  
 975 noisy gradient descent:

$$\begin{aligned}\theta_L^{t+1} &= \Pi_{\Theta} \left[ \theta_L^t + \eta \nabla \mathcal{L}_{D_{\text{pub}} \cup D_{\text{priv}}}(\theta_L^t) + \sqrt{2\eta\sigma^2} W_t \right] & (W_t \sim \mathcal{N}(0, I_d)) \\ \theta_R^{t+1} &= \Pi_{\Theta} \left[ \theta_R^t + \eta \nabla \mathcal{L}_{D_{\text{retain}}}(\theta_R^t) + \sqrt{2\eta\sigma^2} W_t \right] & (W_t \sim \mathcal{N}(0, I_d))\end{aligned}$$

981 Let's divide each optimization step into the following:

$$\begin{aligned}\theta_L^{t,1} &= \theta_L^t + \eta \nabla \mathcal{L}_{D_{\text{pub}} \cup D_{\text{priv}}}(\theta_L^t) + \sqrt{\eta\sigma^2} W_t \\ \theta_R^{t,1} &= \theta_R^t + \eta \nabla \mathcal{L}_{D_{\text{retain}}}(\theta_R^t) + \sqrt{\eta\sigma^2} W_t\end{aligned}$$

986 Therefore, we can write

$$\theta_L^{t+1} = \Pi_{\Theta} \left[ \theta_L^{t,1} + \sqrt{\eta\sigma^2} W_t \right] \quad (7)$$

$$\theta_R^{t+1} = \Pi_{\Theta} \left[ \theta_R^{t,1} + \sqrt{\eta\sigma^2} W_t \right]. \quad (8)$$

991 Let  $\pi_R^t, \pi_R^{t,1}, \pi_L^t, \pi_L^{t,1}$  be the distributions of respectively  $\theta_R^t, \theta_R^{t,1}, \theta_L^t, \theta_L^{t,1}$

994 **The main question we try to tackle here is: what is  $D_{\alpha}(\pi_R^t \parallel \pi_L^t)$  ?**

995 We first compare the distributions  $\pi_R^{t,1}$  and  $\pi_L^{t,1}$ . By composition theorem of the Gaussian mechanism for Rényi Differential privacy (Mironov, 2017), and equivalently for the Rényi divergence, we  
 996 have:

$$\frac{D_{\alpha}(\pi_R^{t,1} \parallel \pi_L^{t,1})}{\alpha} \leq \frac{D_{\alpha}(\pi_R^t \parallel \pi_L^t)}{\alpha} + \frac{\Delta_F^2}{2\sigma^2} \quad (9)$$

1001 where  $\Delta_F$  is the  $l_2$  sensitivity of the gradient update. For the next computations, let  $n_{\text{pub}}$  denote  
 1002 the number of public points,  $n_{\text{forget}}$  denote the number of points to forget, and  $n_{\text{r-priv}}$  denote the  
 1003 number of *remaining* private points in the retain set. Computing the sensitivity in the asymmetric  
 1004 setting yields:

$$\begin{aligned}1005 \Delta_F &= \max_{\theta} \eta \|\nabla \mathcal{L}_{D_{\text{retain}}}(\theta) - \nabla \mathcal{L}_{D_{\text{pub}} \cup D_{\text{priv}}}(\theta)\| \\ 1006 &= \max_{\theta} \eta \left\| \frac{1}{n_{\text{pub}} + n_{\text{r-priv}}} \sum_{d_i \in \text{I} \cup \text{II}} \nabla l(\theta, d_i) - \frac{1}{n_{\text{pub}} + n_{\text{r-priv}} + n_{\text{forget}}} \sum_{d_i \in \text{I} \cup \text{II} \cup \text{III}} \nabla l(\theta, d_i) \right\| \\ 1007 &\leq \eta \left( \frac{1}{n_{\text{pub}} + n_{\text{r-priv}}} - \frac{1}{n_{\text{pub}} + n_{\text{r-priv}} + n_{\text{forget}}} \right) \sum_{d_i \in \text{I} \cup \text{II}} \|\nabla l(\theta, d_i)\| \\ 1008 &\quad + \frac{\eta}{n_{\text{pub}} + n_{\text{r-priv}} + n_{\text{forget}}} \sum_{d_i \in \text{I} \cup \text{II} \cup \text{III}} \|\nabla l(\theta, d_i)\| \\ 1009 &\leq M\eta(n_{\text{pub}} + n_{\text{r-priv}}) \left( \frac{1}{n_{\text{pub}} + n_{\text{r-priv}}} - \frac{1}{n_{\text{pub}} + n_{\text{r-priv}} + n_{\text{forget}}} \right) + \frac{n_{\text{forget}} M \eta}{n_{\text{pub}} + n_{\text{r-priv}} + n_{\text{forget}}} \\ 1010 &\leq \underbrace{\frac{2M\eta n_{\text{forget}}}{n_{\text{pub}} + n_{\text{r-priv}} + n_{\text{forget}}}}_{\varepsilon}\end{aligned}$$

1020 **Lemma A.8.** (Ye & Shokri, 2022) For any distributions  $\xi_t, \xi'_t$  both satisfying  $C_{t,1}$ -LSI, we have:

$$\frac{D_{\alpha}(\xi_t * \mathcal{N}(0, \eta\sigma^2 I), \xi'_t * \mathcal{N}(0, \eta\sigma^2 I))}{\alpha} \leq \frac{D_{\alpha(t)}(\xi_t, \xi'_t)}{\alpha(t)} \left( 1 + \frac{\eta\sigma^2}{C_{t,1}} \right)^{-1}$$

1025 where  $\alpha(t) = \frac{\alpha-1}{1 + \frac{\eta\sigma^2}{C_{t,1}}}$

1026 By combining the data processing inequality (projection) and Lemma A.8, we get the following  
 1027 recurrence inequality:  
 1028

$$\begin{aligned}
 \frac{D_\alpha(\pi_R^{T+1} \|\pi_L^{T+1})}{\alpha} &\leq \left( \frac{D_{\alpha(T)}(\pi_R^T \|\pi_L^T)}{\alpha(T)} + \frac{\varepsilon^2}{2\sigma^2} \right) \left( 1 + \frac{\eta\sigma^2}{C_{T,1}} \right)^{-1} \\
 &= \frac{\varepsilon^2}{2\sigma^2} \left( 1 + \frac{\eta\sigma^2}{C_{T,1}} \right)^{-1} + \frac{D_{\alpha(T)}(\pi_R^T \|\pi_L^T)}{\alpha(T)} \left( 1 + \frac{\eta\sigma^2}{C_{T,1}} \right)^{-1} \\
 &\leq \frac{\varepsilon^2}{2\sigma^2} \left( 1 + \frac{\eta\sigma^2}{C_{T,1}} \right)^{-1} + \left( \frac{D_{\alpha(T-1)}(\pi_R^T \|\pi_L^T)}{\alpha(T-1)} + \frac{\varepsilon^2}{2\sigma^2} \right) \left( 1 + \frac{\eta\sigma^2}{C_{T,1}} \right)^{-1} \left( 1 + \frac{\eta\sigma^2}{C_{T-1,1}} \right)^{-1} \\
 &\leq \frac{\varepsilon^2}{2\sigma^2} [B(T) + B(T-1)] + B(T-2) \left( \frac{D_{\alpha(T-2)}(\pi_R^T \|\pi_L^T)}{\alpha(T-2)} + \frac{\varepsilon^2}{2\sigma^2} \right) \\
 &\quad \text{(where } B(t) = \prod_{k=t}^T \left( 1 + \frac{\eta\sigma^2}{C_{k,1}} \right)^{-1} \text{)} \\
 &\leq \frac{\varepsilon^2}{2\sigma^2} \sum_{i=1}^T B(i) + B(0) \left( \frac{D_{\alpha(0)}(\pi_R^T \|\pi_L^T)}{\alpha(0)} + \frac{\varepsilon^2}{2\sigma^2} \right) \\
 &\leq \frac{\varepsilon^2}{2\sigma^2} \sum_{i=0}^T B(i) \quad \text{(since } D_{\alpha(t)}(\pi_0 \|\pi_0) = 0 \text{)} \\
 &= \frac{\varepsilon^2}{2\sigma^2} \sum_{t=0}^T \prod_{t'=t}^T \left( 1 + \frac{\eta\sigma^2}{C_{t',1}} \right)^{-1}
 \end{aligned}$$

1050 The upper bound on the log Sobolev constants can be tracked in a similar fashion as in Proposition  
 1051 A.1 because of the projection onto the compact set  $\Theta$ .  $\square$   
 1052

#### 1053 A.4 PROOF OF THEOREM 3.3

1055 **Proposition.** *Assuming the data generating distributions share the same support, that the weight  
 1056 space  $\Theta$  is compact and that the loss is  $M$ -Lipschitz wrt  $\theta$ , we have the following upper bound on the  
 1057 generalization error on the private data after performing  $K$  iterations of unlearning, and initializing  
 1058 a weight  $\theta_0$  from  $\pi_L^T$ :*

$$\begin{aligned}
 \mathbb{E}_{\theta \sim \pi_U} [\mathbb{E}_{x \sim P_{\text{priv}}} [\mathcal{L}(\theta, x)]] &\leq \underbrace{\exp \left( \frac{n_{\text{pub}}}{n_{\text{pub}} + n_{\text{retain}}} D_\infty(P_{\text{priv}} \| P_{\text{pub}}) \right)}_{\text{distribution mismatch penalty}} \mathbb{E}_{\theta \sim \pi_R} [\mathbb{E}_{d \sim P_{\text{train}}} [\mathcal{L}(\theta, d)]] + \\
 &\quad M \times \text{diam}(\Theta) \times \underbrace{\sqrt{\frac{1}{2} D_\alpha(\pi_R \|\pi_U)}}_{\text{unlearning approximation error}}
 \end{aligned}$$

1067 where  $D_\infty(P \| Q) = \log \left( \text{ess sup}_{x \sim Q} \frac{p(x)}{q(x)} \right)$  is the infinite Rényi divergence (worst case regret (Er-  
 1068 ven & Harremoës, 2014)) and  $p_{\text{train}}$  denotes the mixture of distributions  $D_{\text{pub}}$  and  $D_{\text{priv}}$  used for  
 1069 training the model.

1071 In order to prove Theorem 3.3, we will use the following quantities to define a set of preliminary  
 1072 lemmas.

##### 1074 A.4.1 PERFORMANCE ON THE TRAINING DISTRIBUTION MIXTURE

1076 **Definition A.1** (Wasserstein distance). *The Wasserstein-1 distance is defined as*

$$W_1(\mu, \nu) = \inf_{\gamma \in \Pi(\mu, \nu)} \int_{\mathcal{X} \times \mathcal{X}} d(x, y) d\gamma(x, y),$$

1077 where:  
 1078  
 1079

- $\mu$  and  $\nu$  are probability measures on a metric space  $(\mathcal{X}, d)$ ,
- $d(x, y)$  is the distance between points  $x, y \in \mathcal{X}$ ,
- $\Pi(\mu, \nu)$  is the set of all couplings of  $\mu$  and  $\nu$ , i.e., the set of joint distributions  $\gamma$  on  $\mathcal{X} \times \mathcal{X}$  such that the marginals of  $\gamma$  are  $\mu$  and  $\nu$ :

$$\int_{\mathcal{X}} \gamma(x, y) dy = \mu(x), \quad \int_{\mathcal{X}} \gamma(x, y) dx = \nu(y).$$

**Definition A.2** (Total Variation Distance). Let  $P$  and  $Q$  be two probability measures on a measurable space  $(\Omega, \mathcal{F})$ . The **total variation distance** between  $P$  and  $Q$  is defined as

$$TV(P, Q) = \sup_{A \in \mathcal{F}} |P(A) - Q(A)| \quad (10)$$

$$= \frac{1}{2} \int_{\Omega} |dP - dQ| \quad (11)$$

$$= \frac{1}{2} \|P - Q\|_{TV}. \quad (12)$$

**Theorem A.1.** (Kantorovich Rubinstein's duality, (Villani et al., 2009), Theorem 5.10) If  $\mu, \nu$  have a bounded support  $\Omega$ , then

$$W_1(\mu, \nu) = \sup_{\|h\|_L \leq 1} \mathbb{E}_{x \sim \mu}[h(x)] - \mathbb{E}_{y \sim \nu}[h(y)], \quad (13)$$

where  $\|h\|_L \leq 1$  denotes the set of 1-Lipschitz functions on  $\Omega$

Let  $f : \Theta \rightarrow \mathbb{R}$  such that  $f(\theta) = \mathbb{E}_{D \sim P_{\text{train}}}[\mathcal{L}_D(\theta)]$ , where  $P_{\text{train}}$  denotes the training data distribution (a mixture of  $P_{\text{priv}}$  and  $P_{\text{pub}}$ ). Since  $\mathcal{L}(\cdot, D)$  is  $M$ -Lipschitz, so is  $f$ . Then, we have that:

$$\begin{aligned} \mathbb{E}_{\substack{\theta \sim \pi_U \\ D \sim P_{\text{train}}}} [\mathcal{L}(\theta, D)] - \mathbb{E}_{\substack{\theta \sim \pi_R \\ D \sim P_{\text{train}}}} [\mathcal{L}(\theta, D)] &= \mathbb{E}_{\theta \sim \pi_U}[f(\theta)] - \mathbb{E}_{\theta \sim \pi_R}[f(\theta)] \quad (\text{Fubini's theorem}) \\ &\leq M \times W_1(\pi_U, \pi_R) \quad (\text{By Theorem A.1}) \end{aligned}$$

Now, we need to find an upper bound on the 1-Wasserstein distance in terms of the Rényi divergence between  $\pi_R$  and  $\pi_U$ . The following results will be useful in deriving it:

**Proposition A.2.** (Pinsker's inequality) For two probability distributions  $P, Q$ , we have

$$2TV(P, Q)^2 \leq KL(P||Q). \quad (14)$$

**Proposition A.3.** (Monotonicity of Rényi divergence, (Erven & Harremoës, 2014)) For  $1 \leq \alpha_1 \leq \alpha_2$  and probability measures  $P, Q$ ,

$$KL(P||Q) \leq D_{\alpha_1}(P||Q) \leq D_{\alpha_2}(P||Q).$$

The  $KL$  lower bounds any Rényi divergence since it is obtained by the limit  $\alpha \rightarrow 1$ .

**Proposition A.4.** (Upper bounding  $W_1$  with  $TV$  (Gibbs & Su, 2002)) If the distributions  $P, Q$  share a support  $\Omega$  and  $\text{diam}(\Omega) = \sup_{(x,y) \in \Omega \times \Omega} d(x, y)$  is finite, then we have

$$W_1(P, Q) \leq \text{diam}(\Omega)TV(P, Q). \quad (15)$$

Using the results above, we have

$$\begin{aligned} \mathbb{E}_{\theta \sim \pi_U}[f(\theta)] - \mathbb{E}_{\theta \sim \pi_R}[f(\theta)] &\leq MW_1(\pi_U, \pi_R) \\ &\leq M \times \text{diam}(\Theta) \times TV(\pi_U, \pi_R) \\ &\quad (\text{By Proposition A.4 and compactness of } \Theta) \\ &\leq M \times \text{diam}(\Theta) \times \sqrt{\frac{1}{2} KL(\pi_U, \pi_R)} \quad (\text{By Proposition A.3}) \\ &\leq M \times \text{diam}(\Theta) \times \sqrt{\frac{1}{2} D_{\alpha}(\pi_U, \pi_R)} \quad (\text{By Proposition A.3}) \end{aligned}$$

Thus, we obtain that the generalization error of learning + unlearning is upper bounded by:

**Proposition A.5.** Assuming that  $\mathcal{L}$  is  $M$ -Lipschitz, we have

$$\mathbb{E}_{\theta \sim \pi_U} [\mathbb{E}_{D \sim P_{\text{train}}}[\mathcal{L}(\theta, D)]] \leq \mathbb{E}_{\theta \sim \pi_R} [\mathbb{E}_{D \sim P_{\text{train}}}[\mathcal{L}(\theta, D)]] + M \times \text{diam}(\Theta) \times \sqrt{\frac{1}{2} D_{\alpha}(\pi_U, \pi_R)} \quad (16)$$

1134 A.4.2 ADAPTING THE BOUND TO THEOREM 3.3  
1135

1136 We would like to evaluate the performance of the model obtained after unlearning. Proposition  
1137 A.5 provides a generalization bound on a mixture of distributions, namely on public data + pri-  
1138 vate data. In most practical scenarios, one would want to quantify the "lost" performance on  
1139 private data after forgetting one of its subsets. Thus, we would like to upper bound the quantity  
1140  $\mathbb{E}_{\pi_U} [\mathbb{E}_{D \sim P_{\text{priv}}} [\mathcal{L}_D(\theta)]]$ . The training data distribution used for either retraining or unlearning can  
1141 be considered as generated from a mixture of the distributions  $I$  and  $II$ . Assuming the sampling  
1142 proportions for training are consistent, one can write that the data distribution used in retraining is

$$1143 P_{\text{train}} = \frac{n_{\text{pub}}}{n_{\text{pub}} + n_{\text{r-priv}}} P_{\text{pub}} + \frac{n_{\text{r-priv}}}{n_{\text{pub}} + n_{\text{r-priv}}} P_{\text{priv}}.$$

1146 Fix any  $\theta \in \Theta$ . We have that

$$\begin{aligned} 1148 \mathbb{E}_{\mathcal{D} \sim P_{\text{train}}} [\mathcal{L}(\theta, \mathcal{D})] &= \frac{n_{\text{pub}}}{n_{\text{pub}} + n_{\text{r-priv}}} \mathbb{E}_{\mathcal{D} \sim P_{\text{pub}}} [\mathcal{L}(\theta, \mathcal{D})] + \frac{n_{\text{r-priv}}}{n_{\text{pub}} + n_{\text{r-priv}}} \mathbb{E}_{\mathcal{D} \sim P_{\text{priv}}} [\mathcal{L}(\theta, \mathcal{D})] \\ 1151 \mathbb{E}_{\mathcal{D} \sim P_{\text{priv}}} [\mathcal{L}(\theta, \mathcal{D})] &= \int p_{\text{priv}}(x) \mathcal{L}(\theta, x) dx \\ 1154 &= \int p_{\text{train}}(x) \frac{p_{\text{priv}}(x)}{p_{\text{train}}(x)} \mathcal{L}(\theta, x) dx \\ 1156 &= \mathbb{E}_{x \sim P_{\text{train}}} \left[ \frac{p_{\text{priv}}(x)}{p_{\text{train}}(x)} \mathcal{L}(\theta, x) \right] \\ 1158 &\leq \mathbb{E}_{d \sim P_{\text{train}}} [\text{ess sup}_{x \in \text{Supp}(P_{\text{pub}}) \cup \text{Supp}(P_{\text{priv}})} \frac{p_{\text{priv}}(x)}{p_{\text{train}}(x)} \mathcal{L}(\theta, d)] \\ 1160 &\leq \text{ess sup}_{x \in \text{Supp}(P_{\text{pub}}) \cup \text{Supp}(P_{\text{priv}})} \frac{p_{\text{priv}}(x)}{p_{\text{train}}(x)} \mathbb{E}_{d \sim P_{\text{train}}} [\mathcal{L}(\theta, d)] \\ 1162 &\leq \exp(D_\infty(P_{\text{priv}}, P_{\text{train}})) \mathbb{E}_{d \sim P_{\text{train}}} [\mathcal{L}(\theta, d)]. \end{aligned}$$

1164 Moreover, we have by convexity of the Rényi divergence (Erven & Harremoës, 2014) in its second  
1165 argument that

$$1167 D_\infty(P_{\text{priv}} \| P_{\text{train}}) \leq \frac{n_{\text{pub}}}{n_{\text{pub}} + n_{\text{r-priv}}} (P_{\text{priv}} \| P_{\text{pub}}).$$

1169 Thus we also have

$$1171 \mathbb{E}_{d \sim P_{\text{priv}}} [\mathcal{L}(\theta, d)] \leq \exp \left( \frac{n_{\text{pub}}}{n_{\text{pub}} + n_{\text{r-priv}}} D_\infty(P_{\text{priv}} \| P_{\text{pub}}) \right) \mathbb{E}_{d \sim P_{\text{train}}} [\mathcal{L}(\theta, d)]. \quad (17)$$

1174 Thus, we can adapt proposition A.5 to evaluate the risk *only* on private data. Note that so far, the  
1175 only assumption made on the difference between the data generating distributions I and II is that  
1176 they share the same support. The following bound might be refined with additional assumptions,  
1177 such as covariate shift or conditional shift.

1178 We can thus take the expectation of  $\theta$  with respect to  $\pi_U$  to get

$$1180 \mathbb{E}_{\theta \sim \pi_U} [\mathbb{E}_{d \sim P_{\text{priv}}} [\mathcal{L}(\theta, d)]] \leq \exp \left( \frac{n_{\text{pub}}}{n_{\text{pub}} + n_{\text{r-priv}}} D_\infty(P_{\text{priv}} \| P_{\text{pub}}) \right) \mathbb{E}_{\theta \sim \pi_U} [\mathbb{E}_{d \sim P_{\text{train}}} [\mathcal{L}(\theta, d)]],$$

1182 and using proposition A.5 to upper bound  $\mathbb{E}_{\theta \sim \pi_U} [\mathbb{E}_{d \sim P_{\text{train}}} [\mathcal{L}(\theta, d)]]$ , we prove proposition 3.3:

$$\begin{aligned} 1184 \mathbb{E}_{\theta \sim \pi_U} [\mathbb{E}_{x \sim P_{\text{priv}}} [\mathcal{L}(\theta, x)]] &\leq \exp \left( \frac{n_{\text{pub}}}{n_{\text{pub}} + n_{\text{r-priv}}} D_\infty(P_{\text{priv}} \| P_{\text{pub}}) \right) \mathbb{E}_{\theta \sim \pi_R} [\mathbb{E}_{d \sim P_{\text{train}}} [\mathcal{L}(\theta, d)]] + \\ 1186 &\quad M \times \text{diam}(\Theta) \times \sqrt{\frac{1}{2} D_\alpha(\pi_R \| \pi_U)}. \end{aligned}$$

1188

**Algorithm 1** Training with Projected Noisy Gradient Descent (PNGD)

1189

```

1:  $\theta_0 \sim \pi_0$  ▷ Sample from initialization distribution
2: for  $t = 0$  to  $T - 1$  do
3:    $g_t \leftarrow \nabla_{\theta} L_D(\theta_t)$  ▷ Compute gradient on full dataset
4:    $\xi_t \sim \mathcal{N}(0, 2\eta\sigma^2 I_d)$  ▷ Sample Gaussian noise
5:    $\theta_{t+1} \leftarrow \Pi_{\Theta}[\theta_t - \eta g_t + \xi_t]$  ▷ Update and project
6: end for
7: return  $\theta_T$ 

```

1190

1191

1192

1193

1194

1195

1196

1197

1198

**Algorithm 2** Langevin Unlearning

1199

```

1:  $\theta_0^U \leftarrow \theta_T$  ▷ Initialize from trained model
2: for  $k = 0$  to  $K - 1$  do
3:    $g_k \leftarrow \nabla_{\theta} L_{D_{\text{retain}}}(\theta_k^U)$  ▷ Compute gradient on retain set only
4:    $\xi_k \sim \mathcal{N}(0, 2\eta\sigma^2 I_d)$  ▷ Sample Gaussian noise
5:    $\theta_{k+1}^U \leftarrow \Pi_{\Theta}[\theta_k^U - \eta g_k + \xi_k]$  ▷ Update and project
6: end for
7: return  $\theta_K^U$ 

```

1200

1201

1202

1203

1204

1205

1206

1207

1208

**A.5** LANGEVIN UNLEARNING PSEUDO-CODE

1209

1210

1211

1212

**A.6** DOMAINNET DATA

1213

1214

1215

1216

The following is a snippet of samples from the DomainNet dataset, where we extracted two domains, Clipart and Quickdraw. The classes are aggregated into 24 meta-classes Table 3, following (Peng et al., 2019).

1217

1218

1219

1220

1221

1222

1223

1224

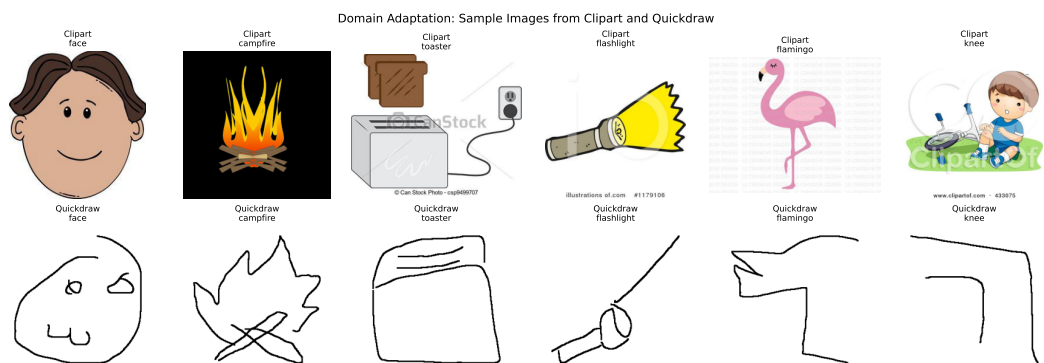
1225

1226

1227

1228

1229



1230

1231

1232

1233

1234

1235

1236

1237

Figure 4: The two domains of public and private data used for Sections 4.1 and 4.2 (Peng et al., 2019). Both datasets share the same number of classes, with Clipart being a collection of stylized images representing the private data, and Quickdraw representing a collection of hand-draw sketches.

1238

1239

1240

1241

**A.7** DETAILS ABOUT THE RÉNYI ESTIMATION**A.7.1** NEURAL RÉNYI ESTIMATION

Following the works of Birrell et al. (2021; 2023), two variational representations of the Rényi divergence between two distributions  $P, Q$  have been proposed. The first draws inspiration from the Donsker–Varadhan dual representation (Donsker & Varadhan, 1975) of the KL divergence:

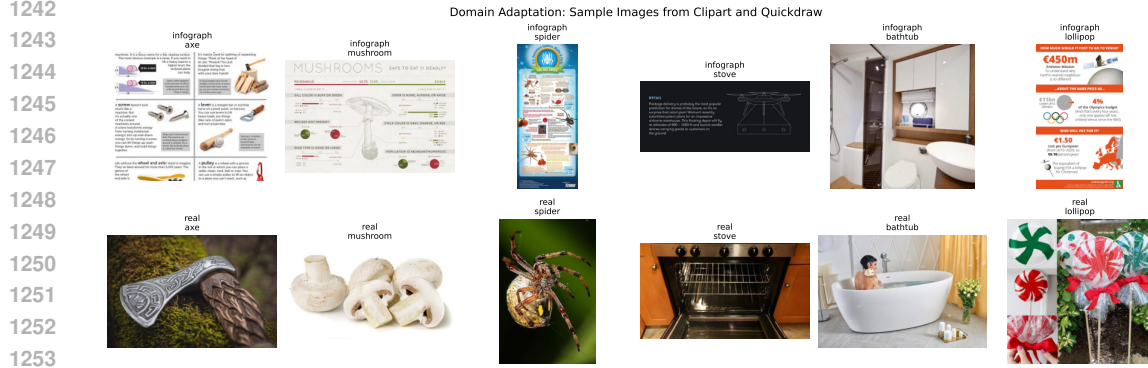


Figure 5: The two domains of public and private data used for Section 4.2 (Peng et al., 2019). Both datasets share the same number of classes, with Infograph being a collection of stylized images representing the public data, and Real representing a collection of real-life images.

**Theorem A.2** (Donsker–Varadhan Rényi divergence (Birrell et al., 2021)). *Let  $P, Q$  be two distributions on  $(\Omega, \mathcal{M})$  and  $\alpha \in \mathbb{R}$ ,  $\alpha \neq 0, 1$ . Then, for any set of functions  $\Phi$  with  $\mathcal{M}_b(\Omega) \subset \Phi \subset \mathcal{M}(\Omega)$ ,*

$$\frac{D_\alpha(P\|Q)}{\alpha} = \sup_{\phi \in \Phi} \left\{ \frac{1}{\alpha-1} \log \int e^{(\alpha-1)\phi} dP - \frac{1}{\alpha} \log \int e^{\alpha\phi} dQ \right\}. \quad (18)$$

*If in addition  $(\Omega, \mathcal{M})$  is a metric space with the Borel  $\sigma$ -algebra, then Eq. (18) holds for all  $\Phi$  satisfying  $\text{Lip}_b \subset \Phi \subset \mathcal{M}(\Omega)$ , where  $\text{Lip}_b$  denotes the set of bounded Lipschitz functions.*

Here,  $\mathcal{M}(\Omega)$  denotes the space of measurable real-valued functions on  $\Omega$ , and  $\mathcal{M}_b(\Omega)$  the subspace of bounded functions.

While this representation allows sample-based estimation, it involves exponential terms that yield high-variance estimates in practice. To mitigate this issue, Birrell et al. (2023) proposed a convex conjugate formulation:

**Theorem A.3** (Convex conjugate Rényi divergence (Birrell et al., 2023)). *Let  $P, Q$  be probability distributions supported on  $\Omega$ , with  $P \ll Q$ , and let  $\mathcal{M}_b(\Omega)$  denote the space of bounded measurable functions. Then, for all  $\alpha \in (0, +\infty) \setminus \{1\}$ ,*

$$\frac{D_\alpha(P\|Q)}{\alpha} = \sup_{g \in \mathcal{M}_b(\Omega), g < 0} \int g dQ + \frac{1}{\alpha-1} \int |g|^{\frac{\alpha-1}{\alpha}} dP + \frac{1}{\alpha} (\log \alpha + 1). \quad (19)$$

This convex conjugate formulation removes the exponential dependence and provides more stable numerical estimates, making it preferable for our setting.

**Neural network parameterization.** To approximate  $\Phi = \{g \in \mathcal{M}(\Theta) : g < 0\}$  we use the class  $g_\theta$  of two-layer MLPs with spectral normalization (Miyato et al., 2018), LeakyReLU activations, and a polysoftplus output activation as in Birrell et al. (2023). The polysoftplus activation offers superior numerical stability compared to ReLU. It is defined as

$$\text{polysoftplus}(x) = - \left( \frac{1}{1-x} \mathbf{1}_{x<0} + (1+x) \mathbf{1}_{x \geq 0} \right). \quad (20)$$

The discriminator network  $g_\theta$  is trained to maximize the variational bound in Eq. (4) using samples  $\{\theta_i^U\}_{i=1}^N \sim \pi_U^K$  and  $\{\theta_j^R\}_{j=1}^N \sim \pi_R^{T+K}$ . The optimization objective becomes:

$$\max_{\theta} \left\{ \frac{1}{N} \sum_{j=1}^N g_\theta(\theta_j^R) + \frac{1}{\alpha-1} \frac{1}{N} \sum_{i=1}^N |g_\theta(\theta_i^U)|^{\frac{\alpha-1}{\alpha}} + \frac{1}{\alpha} (\log \alpha + 1) \right\}. \quad (21)$$

To reduce estimator variance, we repeat the discriminator training five times with different random initializations and report the average. We use a learning rate of value 0.0001 with Adam optimizer (Kingma & Ba, 2017), and train the discriminators for 30000 epochs with batch size  $b = 6000$ .

1296 Table 3: Class aggregation for experimental dataset. Individual classes are grouped into 24 super-  
1297 classes.  
1298

1299 <b>Superclass</b>	1300 <b>Individual Classes</b>
1300 Furniture	1301 bathtub, bed, bench, ceiling fan, chair, chandelier, couch, door, dresser, fence, fireplace, floor lamp, hot tub, ladder, lantern, 1302 mailbox, picture frame, pillow, postcard, see saw, sink, sleeping bag, stairs, stove, streetlight, suitcase, swing set, table, 1303 teapot, toilet, toothbrush, toothpaste, umbrella, vase, wine glass
1303 Mammal	1304 bat, bear, camel, cat, cow, dog, dolphin, elephant, giraffe, hedgehog, horse, kangaroo, lion, monkey, mouse, panda, pig, 1305 rabbit, raccoon, rhinoceros, sheep, squirrel, tiger, whale, zebra
1305 Tool	1306 anvil, axe, bandage, basket, boomerang, bottlecap, broom, bucket, compass, drill, dumbbell, hammer, key, nail, paint can, 1307 passport, pliers, rake, rifle, saw, screwdriver, shovel, skateboard, stethoscope, stitches, sword, syringe, wheel
1307 Cloth	1308 belt, bowtie, bracelet, camouflage, crown, diamond, eyeglasses, flip flops, hat, helmet, jacket, lipstick, necklace, pants, 1309 purse, rollerskates, shoe, shorts, sock, sweater, t-shirt, underwear, wristwatch
1308 Electricity	1310 calculator, camera, cell phone, computer, cooler, dishwasher, fan, flashlight, headphones, keyboard, laptop, light bulb, 1311 megaphone, microphone, microwave, oven, power outlet, radio, remote control, spreadsheet, stereo, telephone, television, 1312 toaster, washing machine
1310 Building	1311 The Eiffel Tower, The Great Wall, barn, bridge, castle, church, diving board, garden, garden hose, golf club, hospital, 1312 house, jail, lighthouse, pond, pool, skyscraper, square, tent, waterslide, windmill
1312 Office	1313 alarm clock, backpack, binoculars, book, calendar, candle, clock, coffee cup, crayon, cup, envelope, eraser, map, marker, 1314 mug, paintbrush, paper clip, pencil, scissors
1313 Human Body	1315 arm, beard, brain, ear, elbow, eye, face, finger, foot, goatee, hand, knee, leg, moustache, mouth, nose, skull, smiley face, 1316 toe, tooth
1315 Road Transportation	1317 ambulance, bicycle, bulldozer, bus, car, firetruck, motorbike, pickup truck, police car, roller coaster, school bus, tractor, 1318 train, truck, van
1317 Food	1319 birthday cake, bread, cake, cookie, donut, hamburger, hot dog, ice cream, lollipop, peanut, pizza, popsicle, sandwich, steak
1318 Nature	1320 beach, cloud, hurricane, lightning, moon, mountain, ocean, rain, rainbow, river, snowflake, star, sun, tornado
1319 Cold Blooded	1321 crab, crocodile, fish, frog, lobster, octopus, scorpion, sea turtle, shark, snail, snake, spider
1320 Music	1322 cello, clarinet, drums, guitar, harp, piano, saxophone, trombone, trumpet, violin
1322 Fruit	1323 apple, banana, blackberry, blueberry, grapes, pear, pineapple, strawberry, watermelon
1323 Sport	1324 baseball, baseball bat, basketball, flying saucer, hockey puck, hockey stick, snorkel, soccer ball, tennis racquet, yoga
1324 Tree	1325 bush, cactus, flower, grass, house plant, leaf, palm tree, tree
1325 Bird	1326 bird, duck, flamingo, owl, parrot, penguin, swan
1326 Vegetable	1327 asparagus, broccoli, carrot, mushroom, onion, peas, potato, string bean
1327 Shape	1328 circle, hexagon, line, octagon, squiggle, triangle, zigzag
1328 Kitchen	1329 fork, frying pan, hourglass, knife, lighter, matches, spoon, wine bottle
1329 Water Transportation	1330 aircraft carrier, canoe, cruise ship, sailboat, speedboat, submarine
1330 Sky Transportation	1331 airplane, helicopter, hot air balloon, parachute
1331 Insect	1332 ant, bee, butterfly, mosquito
1332 Others	1333 The Mona Lisa, angel, animal migration, campfire, cannon, dragon, feather, fire hydrant, mermaid, snowman, stop sign, 1334 teddy-bear, traffic light

1336 This procedure used  $N = 30,000$  model samples, which makes it computationally intensive and  
1337 better suited for theoretical validation than for large-scale empirical benchmarking. Although reg-  
1338 ularization and repeated runs alleviate variance, Rényi divergence estimation remains a statistically  
1339 challenging task. Developing scalable and lower-variance estimators is therefore an important di-  
1340 rection for future work.

#### 1343 A.7.2 SAMPLING FROM $\pi_U^K$ AND $\pi_R^{T+K}$

1345 We conduct experiments on the DomainNet dataset (24-class image classification) Fig. 4. We  
1346 choose the domain Clipart as the private data domain, which are stylized images, and Quick-  
1347 draw, a collection of hand-drawn sketches as the public domain. Image embeddings are extracted  
1348 using DinoV2 (Oquab et al., 2024), a self-supervised vision transformer. We specifically use  
1349 vit\_small\_patch16\_224\_dino (Caron et al., 2021). All images are resized to  $224 \times 224$  prior to feature  
extraction.

1350 On these embeddings, we train 30,000 linear classifiers on the full dataset  $D = D_{\text{pub}} \cup D_{\text{priv}}$   
 1351 for  $T = 20$  iterations, and subsequently fine-tune them on the retain set  $D_r = D \setminus D_{\text{forget}}$  for  
 1352  $K \in \{1, 5, 10, 15\}$  additional iterations. This procedure yields 30,000 samples from the unlearning  
 1353 distribution  $\pi_U^K$ .

1354 For comparison, we train another 30,000 linear classifiers directly on the retain set  $D_r$  for  $T + K$   
 1355 iterations, producing samples from the retraining distribution  $\pi_R^{T+K}$ . All models are trained using  
 1356 the same projected noisy gradient descent (PNGD) update with noise scale  $\sigma = 0.01$ , learning rate  
 1357  $\eta = 0.001$ , batch size  $b = 1024$ , and radius  $R = 1.0$  using SGD.

1358 To assess robustness across dataset splits, we fix the total training set size to  $N_{\text{train}} = 42,000$ , and  
 1359 vary the public and forget set sizes as  $(|D_{\text{pub}}|, |D_{\text{forget}}|) \in \{(10,000, 12,000), (15,000, 7,000),$   
 1360 and  $(20,000, 2,000)\}$ . The remaining private data in the retain set is fixed to have size 20,000. The  
 1361 resulting divergence estimates are reported in Figs. 2a and 2b.

1362 **A.7.3 PSEUDO-CODE**

---

1363 **Algorithm 3** Rényi Divergence Estimation via Variational Representation

---

1364 1: **Input:** Samples  $\{\theta_i^R\}_{i=1}^N \sim \pi_R^{T+K}$ ,  $\{\theta_j^U\}_{j=1}^N \sim \pi_U^K$ , order  $\alpha$ , discriminator architecture  
 1365 2: Initialize discriminator network  $g_\phi$  with spectral normalization  
 1366 3: **for** epoch = 1 to num\_epochs **do**  
 1367 4:     Sample minibatch from retraining samples  $\{\theta_i^R\}$   
 1368 5:     Sample minibatch from unlearning samples  $\{\theta_j^U\}$   
 1369 6:     Compute variational objective:

$$1370 \quad \mathcal{L} = \frac{1}{N} \sum_{i=1}^N g_\phi(\theta_i^R) + \frac{1}{\alpha-1} \frac{1}{N} \sum_{j=1}^N |g_\phi(\theta_j^U)|^{\frac{\alpha-1}{\alpha}} + \frac{1}{\alpha} (\log \alpha + 1) \quad (22)$$

1371 7:     Update  $\phi$  to maximize  $\mathcal{L}$  via gradient ascent  
 1372 8: **end for**  
 1373 9: **Output:** Estimated divergence  $\widehat{D}_\alpha(\pi_U^K \parallel \pi_R^{T+K}) = \widehat{\mathcal{L}}^{1/\alpha}$

---

1380 **A.8 EVALUATION WITH U-LiRA**

1381 **A.8.1 U-LiRA DETAILS**

1382 U-LiRA, introduced by Hayes et al. (2025) as an adaptation of the LiRA membership inference  
 1383 attack (Carlini et al., 2021) to the unlearning setting, formalizes unlearning evaluation as a binary  
 1384 hypothesis test. The goal is to distinguish between two distributions over model parameters: the  
 1385 unlearning distribution  $\pi_U^K$ , obtained by training on the full dataset and subsequently applying the  
 1386 target unlearning algorithm to remove the influence of the forget set, and the retraining distribution  
 1387  $\pi_R^{T+K}$ , obtained by training from scratch without the forget set. Letting  $P(\theta \mid \cdot)$  denote the like-  
 1388 lihood of observing model parameters  $\theta$  under a given distribution, the Neyman–Pearson lemma  
 1389 (Neyman & Pearson, 1933) implies that the most powerful test for this discrimination problem is  
 1390 achieved by thresholding the likelihood ratio

$$1391 \quad \frac{P(\theta \mid \pi_U^K)}{P(\theta \mid \pi_R^{T+K})}$$

1392 for model parameters  $\theta$ .

1393 Since directly computing  $P(\theta \mid \pi_U^K)$  and  $P(\theta \mid \pi_R^{T+K})$  is infeasible in practice, U-LiRA employs  
 1394 a series of approximations. First, the two distributions are approximated empirically by sampling:  
 1395 the adversary trains  $N$  models under  $\pi_U^K$  (full training followed by unlearning) and  $N$  models under  
 1396  $\pi_R^{T+K}$  (training from scratch without the forget set).

1397 To reduce the sample complexity required for a low-variance estimate, U-LiRA projects models into  
 1398 a one-dimensional representation space via a statistic  $f : \Theta \rightarrow \mathbb{R}$  (since we only run the attack on  
 1399 forget sets of size 1, we follow Hayes et al. (2025) and choose  $f$  to be the model’s confidence score

1404 on the forget example, rescaled by the logit function  $\phi(\omega) = \ln\left(\frac{\omega}{1-\omega}\right)$ ). The test is then conducted  
 1405 on the surrogate likelihood ratio  
 1406

$$\frac{P(f(\theta)|f(\pi_U^K))}{P(f(\theta)|f(\pi_R^{T+K}))}.$$

1407 As a final simplifying approximation, U-LiRA models the projected distributions as Gaussians  
 1408  
 1409

$$f(\pi_U^K) \approx \mathcal{N}(\mu_U, \sigma_U^2), \quad f(\pi_R^{T+K}) \approx \mathcal{N}(\mu_R, \sigma_R^2),$$

1410 where the parameters  $(\mu_U, \sigma_U^2)$  and  $(\mu_R, \sigma_R^2)$  are estimated directly from the  $N$  sample models of  
 1411 each distribution.  
 1412

1413 In 4.3, we presented the attack through the lens of Bayes' rule (following Algorithm 1 of Hayes  
 1414 et al. (2025)), providing a more intuitive explanation for readers less familiar with hypothesis testing  
 1415 concepts.  
 1416

#### 1417 A.8.2 EXPERIMENTAL SETUP

1418 We evaluate unlearning in binary sentiment classification of IMDB reviews (Maas et al., 2011), with  
 1419 Amazon product reviews (Zhang et al., 2015) as public data. Models are 2-layer LSTMs (Hochreiter  
 1420 & Schmidhuber, 1997), trained to minimize cross-entropy loss with projected noisy gradient descent  
 1421 (Gaussian noise variance  $\sigma^2 = 0.01$ , projection onto an  $\ell_2$  ball of radius 100).  
 1422

1423 For each trial, the forget set consists of a 100 datapoints sampled uniformly from the IMDB reviews  
 1424 dataset. Following the U-LiRA framework, we generate 75 model samples from two distributions:  
 1425

- 1426 • **Unlearning distribution**  $\pi_U^K$ : models trained on 25,000 private datapoints plus the forget  
 1427 set for  $T$  epochs, then finetuned without the forget set for  $K$  epochs.
- 1428 • **Retraining distribution**  $\pi_R^{T+K}$ : models trained from scratch on the same 25,000 private  
 1429 datapoints (excluding the forget set) for  $T + K$  epochs.  
 1430

1431 We repeat this sampling process both with and without the inclusion of the 50,000 public datapoints  
 1432 during training and unlearning.  
 1433

1434  
 1435  
 1436  
 1437  
 1438  
 1439  
 1440  
 1441  
 1442  
 1443  
 1444  
 1445  
 1446  
 1447  
 1448  
 1449  
 1450  
 1451  
 1452  
 1453  
 1454  
 1455  
 1456  
 1457